



Inclusive and differential measurements of the $t\bar{t}$ charge asymmetry in pp collisions at $\sqrt{s} = 8$ TeV



CMS Collaboration*

CERN, Switzerland

ARTICLE INFO

Article history:

Received 11 July 2015

Received in revised form 23 February 2016

Accepted 21 March 2016

Available online 29 March 2016

Editor: M. Doser

Keywords:

CMS

Physics

Top quark

Charge asymmetry

ABSTRACT

The $t\bar{t}$ charge asymmetry is measured in proton–proton collisions at a centre-of-mass energy of 8 TeV. The data, collected with the CMS experiment at the LHC, correspond to an integrated luminosity of 19.7 fb^{-1} . Selected events contain an electron or a muon and four or more jets, where at least one jet is identified as originating from b-quark hadronization. The inclusive charge asymmetry is found to be 0.0010 ± 0.0068 (stat) ± 0.0037 (syst). In addition, differential charge asymmetries as a function of rapidity, transverse momentum, and invariant mass of the $t\bar{t}$ system are studied. For the first time at the LHC, the measurements are also performed in a reduced fiducial phase space of top quark pair production, with an integrated result of -0.0035 ± 0.0072 (stat) ± 0.0031 (syst). All measurements are consistent within two standard deviations with zero asymmetry as well as with the predictions of the standard model.

© 2016 CERN for the benefit of the CMS Collaboration. Published by Elsevier B.V. This is an open access article under the CC BY license (<http://creativecommons.org/licenses/by/4.0/>). Funded by SCOAP³.

1. Introduction

The top quark offers an excellent opportunity to search for deviations from the standard model (SM), as its large mass makes it unique among all quarks. A possible hint for new physics in the top quark sector is the discrepancy between the measured $t\bar{t}$ forward–backward asymmetry and the SM expectations, reported by the CDF [1,2] and D0 [3–5] Collaborations at the Tevatron. Although this discrepancy has become smaller as the measurements and SM calculations [6,7] have been refined, it has generated a number of theoretical explanations invoking contributions from physics beyond the SM (BSM). These have in turn led to models based on axigluons or Z' bosons as mediators in the $t\bar{t}$ production process. An overview of the theoretical explanations can be found in Ref. [8] and references therein.

At hadron colliders top quark pairs are produced predominantly in the processes of gluon–gluon fusion and quark–antiquark annihilation. At leading order (LO), the $t\bar{t}$ production is symmetric with respect to the exchange of the top quark and antiquark. At higher orders, QCD radiative corrections to the $q\bar{q} \rightarrow t\bar{t}$ process induce an asymmetry in the differential distributions of top quarks and antiquarks. The interference between initial- and final-state radiation (ISR and FSR) processes, as well as the interference between the Born and box diagrams, generate a correlation between the

direction of the top quark momentum and that of the incoming quark [9]. Similarly, the direction of the top antiquark momentum is related to that of the incoming antiquark. These processes induce a forward–backward asymmetry (A_{FB}) at the Tevatron $p\bar{p}$ collider. The charge-symmetric pp collisions at the CERN LHC result in a different effect. At the LHC, the larger average momentum fraction of the valence quarks leads to an excess of top quarks produced in the forward and backward directions, while the top antiquarks are produced more centrally. This makes the difference in the absolute values of the rapidities¹ of the top quark and antiquark, $\Delta|y| = |y_t| - |y_{\bar{t}}|$, a suitable observable to measure the $t\bar{t}$ charge asymmetry at the LHC experiments. Using the sensitive variable, the charge asymmetry can be defined as

$$A_C = \frac{N^+ - N^-}{N^+ + N^-}, \quad (1)$$

where N^+ and N^- represent the number of events with positive and negative values of $\Delta|y|$, respectively. Theoretical predictions for this observable are of order 1% in the SM [10,11], but its sensitivity to new physics makes measurements of the effect interesting even when the precision is not high enough to establish the existence of the SM charge asymmetry. Both the CMS and ATLAS

¹ The rapidity is defined as $y = (1/2) \ln[(E + p_z)/(E - p_z)]$, where E denotes the particle energy and p_z its momentum component along the counterclockwise beam direction.

* E-mail address: cms-publication-committee-chair@cern.ch.

Collaborations have published results based on the data collected at a centre-of-mass energy $\sqrt{s} = 7$ TeV, which are in agreement with the SM predictions [12–15].

To shed light on the possible existence and the nature of new physics contributions, it is crucial to measure not only the inclusive asymmetry but also A_C as a function of variables magnifying the $t\bar{t}$ charge asymmetry. For this purpose Eq. (1) is modified to consider only events in a specific bin of the given variable.

In this letter, we present an inclusive measurement and three differential measurements of the $t\bar{t}$ charge asymmetry. The three differential variables, which are each sensitive to a different contribution to the charge asymmetry, include the $t\bar{t}$ system rapidity $|y_{t\bar{t}}|$, its transverse momentum $p_T^{t\bar{t}}$, and its invariant mass $m_{t\bar{t}}$. The measurements use the data collected with the CMS experiment in 2012 corresponding to an integrated luminosity of 19.7 fb^{-1} at $\sqrt{s} = 8$ TeV.

The variable $|y_{t\bar{t}}|$ is sensitive to the ratio of the contributions from the $q\bar{q}$ and gg initial states to $t\bar{t}$ production. The charge-symmetric gluon fusion process is dominant in the central region, while $t\bar{t}$ production through $q\bar{q}$ annihilation mostly produces events with the $t\bar{t}$ pair at larger rapidities, which implies an enhancement of the charge asymmetry with increasing $|y_{t\bar{t}}|$ [10].

The ratio of the positive and negative contributions to the overall asymmetry depends on $p_T^{t\bar{t}}$. In the SM the interference between the Born and the box diagrams leads to a positive contribution, while the interference between ISR and FSR results in a negative contribution. The presence of additional hard radiation implies, on average, a higher transverse momentum (p_T) of the $t\bar{t}$ system. Consequently, in events with large values of $p_T^{t\bar{t}}$, the negative contribution from the ISR–FSR interference is enhanced [10].

The charge asymmetry is expected to depend on $m_{t\bar{t}}$ since the contribution of the $q\bar{q}$ initial state process is enhanced for larger values of this variable. It is also sensitive to BSM contributions; new heavy particles could be exchanged between initial quarks and antiquarks and contribute to the $t\bar{t}$ production (see, e.g. Ref. [16] and references therein). The amplitudes associated with these new contributions would interfere with those of the SM processes, and depending on the model they could lead to an increasing $t\bar{t}$ charge asymmetry with increasing $m_{t\bar{t}}$.

Because only a part of the $t\bar{t}$ phase space is experimentally accessible, measurements of the charge asymmetry that are to be compared to theoretical predictions necessarily include an extrapolation to a more well-defined phase space. To this end a fiducial phase space is defined that emulates the restrictions of the measurable phase space while allowing for the calculation of theoretical predictions. This minimizes the need for extrapolation, which can be subject to unpredictable uncertainties if there are significant BSM contributions. An additional extrapolation to the full phase space of top quark pair production is provided as well, which allows for an easier comparison to the results of other measurements and theoretical calculations.

2. CMS detector

The central feature of the CMS apparatus is a superconducting solenoid of 6 m internal diameter, providing a magnetic field of 3.8 T. Within the solenoid volume are a silicon pixel and strip tracker, a lead tungstate crystal electromagnetic calorimeter (ECAL), and a brass and scintillator hadron calorimeter, each composed of a barrel and two endcap sections. The inner tracker measures trajectories of charged particles within the pseudorapidity range $|\eta| < 2.5$, while the calorimeters provide coverage up to $|\eta| = 3.0$. The pseudorapidity is defined as $\eta = -\ln(\tan\theta/2)$, with the polar angle θ being measured relative to the counterclockwise beam direction. The ECAL has an energy resolution of 3% or better for

the range of electron energies relevant for this analysis. Extensive forward calorimetry complements the coverage provided by the barrel and endcap detectors. Muons are measured in the pseudorapidity range $|\eta| < 2.4$ using gas-ionization detectors embedded in the steel flux-return yoke outside the solenoid. Matching muons to tracks measured in the silicon tracker results in a relative p_T resolution for muons with $20 < p_T < 100$ GeV of 1.3–2.0% in the barrel and better than 6% in the endcaps. The p_T resolution in the barrel is better than 10% for muons with p_T up to 1 TeV [17]. A more detailed description of the CMS detector, together with a definition of the coordinate system used and the relevant kinematic variables, can be found in Ref. [18].

3. Simulated samples

For several steps of the measurement, samples of simulated events are used to model both the signal process and the background contributions arising from the production of single top quarks and vector bosons in association with jets (W+jets and Z+jets). An additional background contribution from QCD multijet events is modelled using a template derived from data; see Section 6. Top quark pairs are produced with the next-to-leading order (NLO) generator POWHEG, version 1.0 [19–22], using the CT10 [23] parton distribution functions (PDF). The electroweak production of single top quarks, in the t -channel and in association with a W boson (tW -channel), is simulated using POWHEG and the CTEQ6M PDF set [24]. The production of electroweak vector bosons in association with jets is simulated using MADGRAPH, version 5.1.3.30 [25], and the CTEQ6L1 [24] PDF set.

For the simulation of $t\bar{t}$ and single top quark events the top quark mass is set to 172.5 GeV. For all samples, PYTHIA, version 6.426 [26], is used for the description of the parton showering and hadronization. The simulations include additional proton–proton interactions in the same bunch crossing (in-time pileup) and in earlier/later bunch crossings (out-of-time pileup) with the same frequency of occurrence as observed in the data.

Differential cross section measurements [27] have shown that the p_T spectrum of the top quarks in $t\bar{t}$ events is significantly softer than the one generated by the used simulation programs. To correct for this effect, the simulated $t\bar{t}$ sample is reweighted according to scale factors derived from these measurements.

4. Event selection

The analysis uses $t\bar{t}$ events in which one of the W bosons from a top quark decay subsequently decays into an electron or muon and the corresponding neutrino, and the other W boson decays into a pair of quarks. We therefore select events containing one electron or muon and four or more jets, at least one of which is identified as originating from the hadronization of a bottom quark. To be considered for the offline analysis, the events must pass a single-electron or a single-muon trigger with p_T thresholds of 27 and 24 GeV for the electron and muon, respectively.

The particle-flow (PF) algorithm [28,29] is used to reconstruct electrons, muons, and jets in the event. The algorithm reconstructs and identifies each individual particle with an optimized combination of information from the various elements of the CMS detector. The reconstructed PF candidates are divided into five classes: electrons, muons, photons, charged hadrons, and neutral hadrons.

The primary vertex of the event [30] is identified as the reconstructed vertex with the highest sum of squared transverse momenta of the associated charged particles. For an event to be accepted, the primary vertex must satisfy criteria on its location within the detector volume, as well as on the quality of its reconstruction.

Electron candidates are required to have a transverse momentum larger than 30 GeV and be within $|\eta| < 2.5$, excluding the transition region between the ECAL barrel and endcaps of $1.44 < |\eta_{\text{sc}}| < 1.57$ since the reconstruction of an electron object in this region is not optimal, where η_{sc} is the pseudorapidity of the electron candidate supercluster [31]. Furthermore, electron candidates are selected based on the value of a multivariate discriminant, which combines different variables related to calorimetry and tracking parameters, but also p_{T} and η of the electron candidate. The electron definition also encompasses a conversion rejection method aimed at identifying electrons from photon conversions. Detailed information on the electron reconstruction can be found in Ref. [31].

Muons are required to have $|\eta| < 2.1$ and $p_{\text{T}} > 26$ GeV, with further requirements on the quality of the muon reconstruction and the compatibility with the primary vertex of the event. The η requirement reflects the coverage of the single-muon trigger. Details on the muon reconstruction can be found in Ref. [17].

Additionally, electron and muon candidates must be isolated. The isolation is quantified by the variable I_{rel}^{ℓ} , defined as the sum of reconstructed transverse momenta of nearby PF objects divided by the lepton transverse momentum (p_{T}^{ℓ}), corrected for pileup effects [31] using the effective area (in η - ϕ space) of the lepton and the energy density in the event. Electrons and muons are required to have $I_{\text{rel}}^{\ell} < 0.1$ and < 0.12 , respectively, using isolation cones with radii of 0.3 and 0.4 in η - ϕ space.

Events with additional electrons and muons are vetoed. The lepton veto is based on a looser definition of the lepton identification. In this definition, electrons must have $p_{\text{T}} > 20$ GeV, $|\eta| < 2.5$ and $I_{\text{rel}}^{\ell} < 0.15$, while passing a loose criterion on the value of the multivariate discriminant. Muons are required to have $p_{\text{T}} > 10$ GeV, $|\eta| < 2.5$, and $I_{\text{rel}}^{\ell} < 0.2$.

Jets are clustered from PF particles with the anti- k_{T} [32] algorithm with a distance parameter of 0.5. Charged hadrons identified as originating from pileup vertices are removed before clustering into jets. Further corrections [33] to the jet energy are applied, depending on jet η and p_{T} , the jet area in η - ϕ space, and the median p_{T} density of the event. The selected jets must lie within $|\eta| < 2.5$ and are required to have $p_{\text{T}} > 30$ GeV. The jet p_{T} resolution in data is approximately 10% worse compared to simulations. To account for this, the transverse momenta of jets in the simulated samples are smeared accordingly. Finally, jets from the hadronization of b quarks are identified using the medium working point of the combined secondary vertex algorithm [34]. The b tag identification efficiency of this algorithm for b jets with $p_{\text{T}} > 30$ GeV and $|\eta| < 2.4$ varies between 60 and 70%, while the misidentification rate for jets arising from light quarks or gluons is about 1% [35].

With the applied event selection we find a total of 171 121 events with an electron in the final state, hereafter referred to as the electron+jets channel, and 192 123 events in the muon+jets channel.

5. Definition of a fiducial phase space

Because of the offline event selection, only a subset of the events collected by the CMS detector is used in the analysis. To allow for a comparison of the measurements with the theoretical calculations, an extrapolation to a well-defined phase space needs to be performed. The extrapolation relies on a correct modelling of the ratio of the number of events in the measured phase space to that in the extrapolated one; such a ratio, however, may be affected by new physics. The simple approach, which is extrapolation to the *full phase space* of $t\bar{t}$ production, entails a large dependence on the model assumptions.

As an alternative, a *fiducial phase space* is defined using generator-level selection criteria that mimic the reconstruction-level criteria applied during the nominal selection. The ratio of the number of fiducial events to the number of reconstruction-level selected events, determined from simulation, is then applied to the data to estimate the distribution of an observable in the fiducial region.

Because of the physical and topological similarity of events in the selected and fiducial phase spaces, new physics contributions are expected to affect both in approximately the same way, leaving the ratio unchanged. Thus this extrapolation to the fiducial phase space is nearly model-independent. It should be noted that the desired model-independence is achieved by using a purely multiplicative correction; a prior subtraction of non-fiducial $t\bar{t}$ events in the selected phase space would require a larger reliance on the model assumptions, as there would be no cancellation of uncertainties.

Jets of generated particles in simulated events are used to emulate the selection steps acting on reconstructed jets. Hadron-level particles are clustered into jets using the anti- k_{T} algorithm with a distance parameter of 0.5, as used for the reconstructed jets. The clustering includes charged leptons and neutrinos, except those created in the leptonic decay of W bosons originating from top quarks. It should be noted that the selection criteria for charged leptons are applied only to leptons originating from top quark decays.

Using these objects the following selection requirements are applied. The event needs to contain exactly one electron (or muon) with $p_{\text{T}} > 30$ (26) GeV and $|\eta| < 2.5$ (2.1). Any event that contains an additional electron (or muon) with $p_{\text{T}} > 20$ (10) GeV and $|\eta| < 2.5$ is rejected. At least four generator-level jets with $p_{\text{T}} > 30$ GeV, $|\eta| < 2.5$ are required. The event is rejected if the axes of any such jets have an angular separation of $\Delta R < 0.4$ to the lepton, where $\Delta R = \sqrt{(\Delta\eta)^2 + (\Delta\phi)^2}$ is calculated using the differences in the azimuthal angles ϕ and pseudorapidities η . This criterion serves as an emulation of the lepton isolation criteria, which use similar radii and are hard to implement for theoretical calculations.

The fiducial region contains about 10% of the events of the full phase space. Roughly 50% of the events in the fiducial region pass the selection outlined in Section 4, with the largest inefficiencies caused by the lepton selection and trigger requirements. In comparison, only 1.5% of the events outside the fiducial region fulfil the event selection criteria, making up about 20% of the selected events.

6. Estimation of background contributions

For the estimation of the background contributions we make use of the discriminating power of the transverse mass of the W boson, m_{T}^{W} , and of M_3 , the invariant mass of the combination of three jets that corresponds to the largest vectorially summed p_{T} . This estimation is necessary for the subtraction of the background contributions of the measured data, as described in Section 7. The m_{T}^{W} variable is calculated from the transverse momentum of the charged lepton $\vec{p}_{\text{T}}^{\ell}$ and the missing transverse momentum vector $\vec{p}_{\text{T}}^{\text{miss}}$. The latter is defined as the p_{T} imbalance of the reconstructed PF objects, taking into account the propagation of jet energy corrections to this observable. Its magnitude is referred to as $E_{\text{T}}^{\text{miss}}$. Neglecting the lepton masses, m_{T}^{W} is defined as

$$m_{\text{T}}^{\text{W}} = \sqrt{2(E_{\text{T}}^{\text{miss}} p_{\text{T}}^{\ell} - \vec{p}_{\text{T}}^{\text{miss}} \cdot \vec{p}_{\text{T}}^{\ell})}. \quad (2)$$

The background estimation is made with a binned maximum likelihood fit for each lepton channel. A simultaneous fit in m_{T}^{W} and M_3 is performed in two disjoint data samples, corresponding to

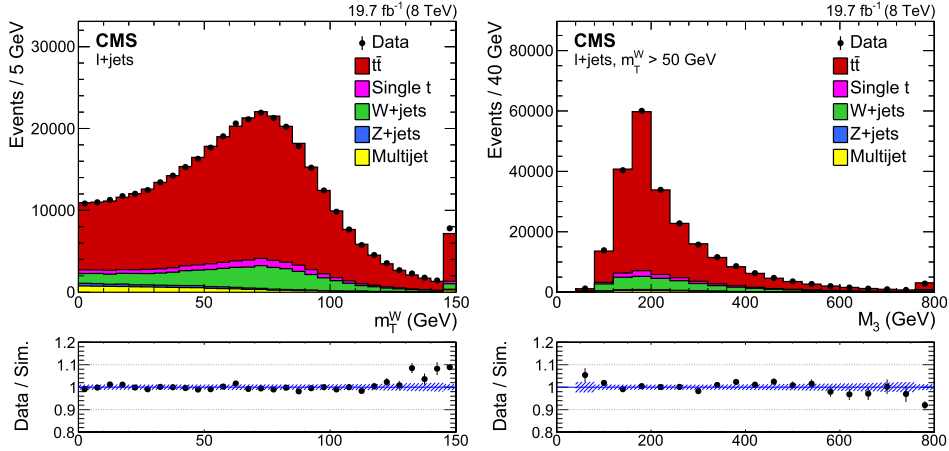


Fig. 1. Comparison of the combined lepton+jets data with simulated contributions for the distributions in m_T^W and M_3 . The simulated signal and background contributions are normalized to the results of the fits in Table 1. The last bin in each histogram includes the overflow values. Additionally, the ratio of the data to the sum of the simulated contributions is shown, with the statistical uncertainties of the simulated contributions (including the uncertainties in the fit) indicated by the blue hatched region. (For interpretation of the references to color in this figure legend, the reader is referred to the web version of this article.)

Table 1

Number of events for background and $t\bar{t}$ contributions from fits to data, along with their statistical uncertainties. The correlations between the individual values have been taken into account for the determination of the uncertainty on the total background yield. The uncertainties quoted for the single top quark and Z+jets backgrounds are driven by the constraints used as inputs for the likelihood fit.

Process	Electron+jets	Muon+jets
Single top quark ($t + tW$)	7016 ± 1328	7302 ± 1663
W+jets	$22\,508 \pm 1460$	$20\,522 \pm 1606$
Z+jets	2345 ± 510	2046 ± 415
QCD multijet	6136 ± 1201	4199 ± 588
Total background	$38\,005 \pm 1491$	$34\,096 \pm 1495$
$t\bar{t}$	$133\,130 \pm 1521$	$158\,058 \pm 1538$
Observed data	171 121	192 123

$m_T^W < 50$ GeV and > 50 GeV. The m_T^W distribution is fitted in the low- m_T^W sample, which is rich in QCD multijet events and yields a good discrimination between the QCD multijet process and processes containing a genuine W boson. The distribution of M_3 is not as dependent on the choice of event sample; it is fitted in the complementary high- m_T^W sample to avoid using the same events for both fits.

For the $t\bar{t}$, W+jets, Z+jets, and single top quark processes, simulated samples are used to model the shapes of the m_T^W and M_3 distributions. The contribution from multijet background events is estimated from data control samples containing nonisolated or poorly identified leptons. Rate constraints corresponding to Gaussian uncertainties of 20% are introduced into the likelihood function for the Z+jets and single top quark processes according to the respective NLO cross sections, while the rates of the other processes are free parameters of the fit. The width of the constraints is motivated by the uncertainties of measurements and theoretical calculations of the corresponding cross sections [36–40]. A detailed description of the fitting procedure can be found in Ref. [41].

Table 1 summarizes the results of the fits. Fig. 1 shows the two variables used for the estimation of the background, with the individual simulated contributions normalized to the results from the fit.

7. Measurement of the $t\bar{t}$ charge asymmetry

The measurement of the $t\bar{t}$ charge asymmetry is based on the reconstructed four-momenta of the t and \bar{t} quarks in each event.

We reconstruct the leptonically decaying W boson from \vec{p}_T^ℓ and \vec{p}_T^{miss} and associate the measured jets in the event with quarks in the $t\bar{t}$ decay chain. The association is done using a likelihood criterion based on the b tagging discriminator values of the jets and the corresponding reconstructed masses of the top quarks and W bosons. The reconstruction procedure is described in detail in Ref. [41].

The reconstructed top quark and antiquark four-momenta are used to obtain the inclusive and differential distributions of $\Delta|y|$, and the charge asymmetry is calculated from the number of entries with $\Delta|y| > 0$ and < 0 . In case of the differential measurements, the asymmetries are calculated separately for the different bins in the kinematic variable V_i , where V_i is either $|y_{t\bar{t}}|$, p_T^{tt} , or $m_{t\bar{t}}$.

To allow for a comparison of the resulting asymmetry and the predictions from theory, the reconstructed distributions of $\Delta|y|$ and the three kinematic variables are corrected for background contributions, resolution, and selection efficiency.

In the first correction step, the distributions of background processes, as used in Section 6, are normalized to the estimated rates (see Table 1) and subtracted from the data, assuming Gaussian uncertainties in the background rates as well as in statistical fluctuations in the background templates. The correlations among the individual background rates are taken into account.

The resulting background-subtracted distributions are translated from the reconstruction level to parton level within the phase space of the selected events. Afterwards, acceptance corrections are applied, correcting either to the fiducial phase space described in Section 5 or to the full phase space. Apart from this last step, the measurements for both phase spaces are identical. After the corrections have been applied, the resulting distributions are independent of the detector and analysis specifications.

The above corrections are obtained by applying an unfolding procedure to the data [42] through a generalized matrix inversion method. In this method, the resolution and selection effects are described by a response matrix R that translates the true spectrum \vec{x} into the measured spectrum $\vec{w} = R\vec{x}$. As reconstruction and selection effects factorize, the response matrix R can be seen as the product of a migration matrix, describing reconstruction effects, and a diagonal matrix containing the selection efficiencies, describing acceptance effects. Both the migration matrix and the selection efficiencies are determined from simulated $t\bar{t}$ events. As the components corresponding to the electron+jets and muon+jets chan-

Table 2

The bin ranges for the individual bins of the differential measurements. Two different choices of binning are used for the distribution of $m_{\bar{t}\bar{t}}$.

Bin	$ y_{\bar{t}} $	$p_T^{\bar{t}}$ (GeV)	$m_{\bar{t}\bar{t}}$ (GeV)	$m_{\bar{t}\bar{t}}$ (GeV)
1	0–0.34	0–41	0–430	0–420
2	0.34–0.75	41–92	430–530	420–500
3	0.75– ∞	92– ∞	530– ∞	500–600
4				600–750
5				750–900
6				900– ∞

nels are found to be very similar, they are combined to yield a method that can be applied to the summed data of both channels. In this combination the individual components are scaled according to the scale factors obtained via the background estimation. The unfolding procedure used in the inclusive measurement, described in detail in Ref. [41], is also used for the two-dimensional distributions of the differential measurements.

This analysis uses 12 bins for the unfolded $\Delta|y|$ distribution in the inclusive measurement and 8 bins for the same distribution in the differential measurements. The unfolded V_i distributions use 3 bins, with one additional measurement being performed using 6 bins in $m_{\bar{t}\bar{t}}$. The additional measurement provides finely grained results in the region of high $m_{\bar{t}\bar{t}}$. The ranges for the bins in these distributions are given in Table 2. It should be noted that the outermost bins of $\Delta|y|$ extend to infinity.

In the corresponding reconstructed spectra the numbers of bins along both axes are doubled, as is recommended for the applied unfolding procedure [42]. The choice of the bin edges for $\Delta|y|$ is different in each bin of V_i , resulting in different amounts of vertical overlap between horizontally neighbouring bins in the two-dimensional distributions (for illustration see the binning in Fig. 2, bottom right).

To limit the magnification of statistical uncertainties due to the unfolding procedure, a regularization is applied that suppresses solutions with large fluctuations between neighbouring bins. The strength of the regularization is determined by minimizing the statistical correlations between bins in the unfolded spectrum. Different strengths are used for the regularization along the sensitive variable within each bin of the kinematic variable. Similarly, the regularization along the kinematic variable is adjusted separately for each bin of the kinematic variable.

Separate migration matrices are used for the inclusive measurement and for each of the differential measurements. Fig. 2 shows the migration matrices for the inclusive measurement and, as an example, for the differential measurement in $m_{\bar{t}\bar{t}}$. For the inclusive measurement the migration matrix describes the migration of selected events from true values of $\Delta|y|$ to the reconstructed values. For the migration matrices of the differential measurements not only the migration between bins of $\Delta|y|$ has to be taken into account, but also the migration between bins of V_i . For a measurement in 3 unfolded bins of V_i these migration matrices feature a grid of 6×3 bins in V_i , with each of these bins representing a 16×8 migration matrix describing the migration between different $\Delta|y|$ values.

The values of $\Delta|y|$ and V_i also affect the probability for an event to fulfil the event selection criteria. The selection efficiencies relative to the full phase space for the inclusive measurement and for the differential measurement in $m_{\bar{t}\bar{t}}$ are depicted in Fig. 2. The selection efficiency of the fiducial phase space is defined by the ratio of all selected events to the events present in the fiducial phase space. It should be noted that the selected events also include events that do not pass the criteria of the fiducial phase space; their influence is implicitly corrected for in the acceptance correction because of the way the selection efficiency is defined.

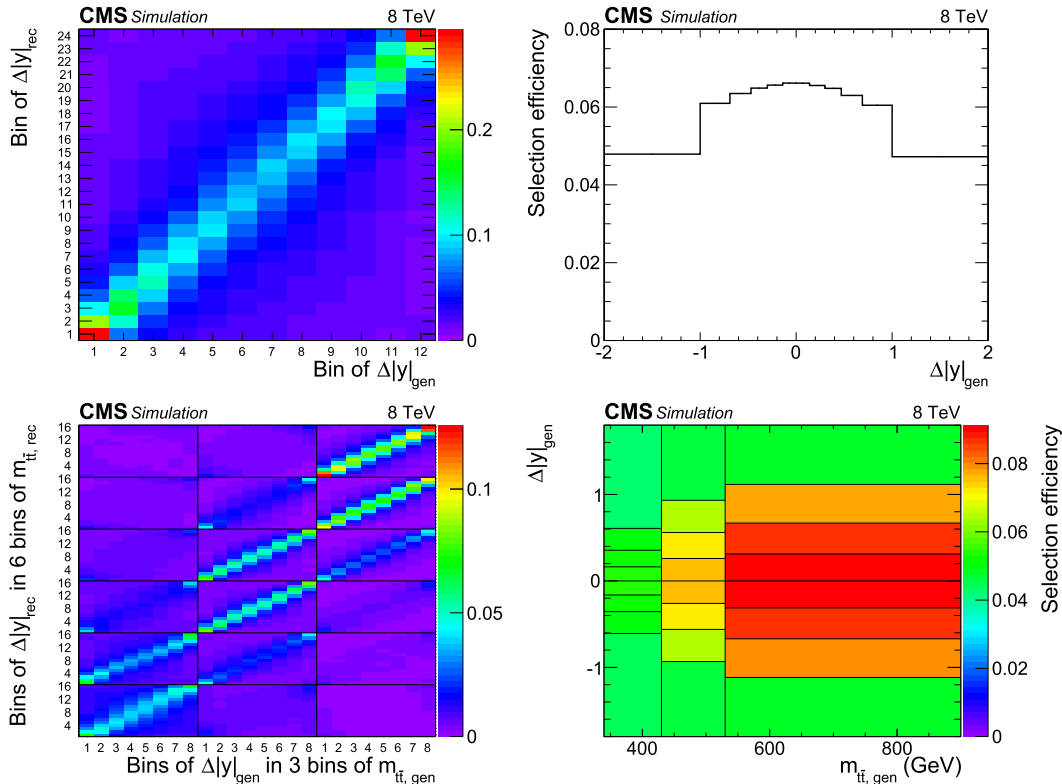


Fig. 2. Migration matrix between generated ($\Delta|y|_{\text{gen}}$) and reconstructed ($\Delta|y|_{\text{rec}}$) rapidity differences (top left) and selection efficiency with respect to the full phase space as a function of $\Delta|y|_{\text{gen}}$ (top right) of the inclusive measurement. Migration matrix (bottom left) and selection efficiency (bottom right) for the measurement differential in $m_{\bar{t}\bar{t}}$.

Thus this correction is multiplicative in nature, which is justified by the inherent similarity of these events to the events that are intended to be measured.

One limiting factor for the precision of the analysis is the presence of sizeable statistical fluctuations in the response matrices as they are obtained from simulated events. To mitigate this effect, one can exploit an approximate symmetry of the response matrix under charge conjugation. For events resulting from a charge-symmetric initial state like gluon–gluon fusion it can be assumed that reconstruction effects also have a predominantly charge-symmetric behaviour. From this reasoning, the symmetry is enforced for this analysis by averaging those bins of the gluon–gluon contribution to the response matrix that correspond to each other under charge conjugation.

The correctness of the unfolding procedure has been verified with pseudo-experiments, each of which provides a randomly generated sample distribution from the templates used in the analysis.

8. Estimation of systematic uncertainties

The measured charge asymmetry A_C is affected by several sources of systematic uncertainty. Effects altering the direction of the reconstructed top quark momenta can change the value of the reconstructed charge asymmetry. Systematic uncertainties with an impact on the differential selection efficiency, as well as variations in the rates and modelling of background contributions, can also bias the result. To evaluate each source of systematic uncertainty, a new background estimation is performed and the measurement is repeated on data using modified simulated samples. The differences in unfolded asymmetries are then used to construct a systematic asymmetry covariance matrix in a loose analogy to statistical covariance matrices. For an uncertainty described by a single systematic shift a covariance of

$$\text{cov}(x, y) = (x - x_{\text{nom}})(y - y_{\text{nom}}) \quad (3)$$

is used, with x and y referring to bins of the asymmetry distribution resulting from the systematic shift and x_{nom} and y_{nom} being the results of the nominal measurement. For uncertainties that are determined using exactly two variations (indexed by 1 and 2) the absolute values of the maximal shifts observed in each result bin, Δx_{max} and Δy_{max} , are determined separately; the covariance is then defined as

$$\text{cov}(x, y) = \Delta x_{\text{max}} \Delta y_{\text{max}} \text{sign}((x_1 - x_2)(y_1 - y_2)). \quad (4)$$

This procedure corresponds to a symmetrization of the largest observed shifts and thus constitutes a more conservative uncertainty estimate than an approach based on a direct analogy with statistical covariance definitions. The covariance matrices of all systematic uncertainties are added up to yield a resultant matrix where the diagonal elements are the variances.

In the following, a summary of the studied sources of systematic uncertainty is given.

The corrections to the jet energy scale and jet energy resolution are varied within their η - and p_T -dependent uncertainties to estimate their effects on the measurement. The effect of variations in the frequency of occurrence of pileup events is determined using reweighted simulated samples. Differences between data and simulations in the b tagging efficiency and the lepton selection efficiency are determined as scale factors that depend on p_T , or η and p_T , respectively. Effects due to uncertainties on these scale factors are studied by varying them as a function of η within their uncertainties and, in the case of the lepton selection efficiency, also as a function of the lepton charge. The effect of lepton charge misidentification is very small and is neglected.

To estimate the influence of a possible mismodelling of the simulated W +jets background, the measurement is repeated using a W +jets template determined from a sideband region in data, defined by an inversion of the requirement of a b -tagged selected jet. The template is reweighted to account for the differences between the signal and sideband regions, which are determined from the simulation.

The uncertainty in the multijet background modelling in the electron+jets channel is determined by replacing the nominal template, which is estimated using two sideband regions defined either by inverted isolation or by inverted identification criteria, with templates derived from only one of the sideband regions each. Meanwhile, in the muon+jets channel, only the template from the isolation-inverted sample can be used, so a conservative estimation of the uncertainty in this background contribution is performed by taking the maximum deviation out of three scenarios where the multijet template is replaced with the $t\bar{t}$ signal template, with the simulated W +jets template, or with a template obtained by inverting the sign of the sensitive variable in the multijet template itself.

In contrast to the other systematic effects, the uncertainty due to the unfolding method is estimated by unfolding simulated samples instead of data. The simulated $t\bar{t}$ events are reweighted to reproduce the observed asymmetries in the differential measurements based on data, and the resulting reconstruction-level spectra are unfolded. The deviations between the unfolded asymmetries and the reweighted true asymmetries are taken to be a measure of the model dependence of the unfolding procedure in the observed point in phase space. The actual uncertainty of each measurement is estimated as the square root of the average squared deviations produced by the unfolding in the three reweighting scenarios corresponding to the three kinematic variables.

To estimate the uncertainty resulting from possible mismodelling of the $t\bar{t}$ signal, samples of simulated $t\bar{t}$ events produced with MADGRAPH are compared to samples produced with POWHEG, both interfaced to PYTHIA for the modelling of the parton shower. In a similar way the impact of a possible mismodelling of parton shower and hadronization is studied by using HERWIG [43,44], as opposed to PYTHIA, for the simulation of the signal, with the hard-scattering matrix element being simulated by either POWHEG or MC@NLO [45]. As a measure of the uncertainty related to the performed reweighting as a function of the top quark p_T , described in Section 3, the measurement is repeated using samples without reweighting. Finally, the impact of variations in the renormalization and factorization scales (μ_R and μ_F) in the simulated $t\bar{t}$ events is determined using dedicated samples generated at scales varied up and down by factors of 2.

The systematic uncertainty on the measured asymmetry from the choice of PDFs for the colliding protons is estimated using the LHAPDF [46] package and the uncertainty in the CT10 [23], MSTW2008 [47], and NNPDF2.1 [48] PDF sets.

The contributions of the different sources of systematic uncertainties to the total uncertainty of the inclusive measurements are summarized in Table 3. The table also shows the ranges of systematic uncertainties in the 3-binned differential measurements to illustrate the magnitudes of the individual contributions. Because the measurements in the two phase spaces differ only by the acceptance corrections, the uncertainties can be seen to behave similarly for the two cases.

9. Results

Table 4 gives the values of the measured inclusive asymmetry at the different stages of the analysis, while the unfolded $\Delta|y|$ distributions for the fiducial and full phase spaces are shown in Fig. 3.

Table 3

Uncertainties for the inclusive measurement of A_C and ranges of uncertainties for the differential measurements using three bins for the kinematic variable. Numbers are given for measurements in the fiducial phase space (fid. PS) and in the full phase space (full PS).

Uncertainty source	Inclusive A_C uncertainty		Differential A_C uncertainty	
	fid. PS	full PS	fid. PS	full PS
Jet energy scale	0.0020	0.0018	0.0009–0.0066	0.0008–0.0063
Jet energy resolution	0.0003	0.0003	0.0005–0.0020	0.0005–0.0020
Pileup	0.0006	0.0006	0.0002–0.0027	0.0003–0.0027
b tagging	0.0009	0.0008	0.0002–0.0033	0.0002–0.0032
Lepton selection efficiency	0.0009	0.0009	0.0005–0.0016	0.0005–0.0017
W+jets background	0.0005	0.0007	0.0003–0.0030	0.0005–0.0025
QCD multijet background	0.0010	0.0009	0.0008–0.0030	0.0011–0.0028
Unfolding	0.0012	0.0022	0.0004–0.0023	0.0011–0.0033
Generator	0.0002	0.0005	0.0008–0.0058	0.0007–0.0043
Hadronization	0.0010	0.0011	0.0007–0.0046	0.0008–0.0040
Top quark p_T reweighting	0.0000	0.0002	0.0000–0.0014	0.0001–0.0015
μ_R and μ_F scales	0.0002	0.0007	0.0008–0.0057	0.0009–0.0064
PDF	0.0002	0.0003	0.0004–0.0014	0.0004–0.0012
Total syst. uncertainty	0.0031	0.0037	0.0043–0.0120	0.0041–0.0115
Statistical uncertainty	0.0072	0.0068	0.0078–0.0181	0.0078–0.0172
Total uncertainty	0.0078	0.0077	0.0094–0.0217	0.0094–0.0207

Table 4

The measured inclusive asymmetry at the different stages of the analysis and the corresponding theoretical predictions from the SM.

	Asymmetry (A_C)
Reconstructed	0.0036 ± 0.0017 (stat)
Background-subtracted	0.0008 ± 0.0023 (stat)
Corrected for migration effects	-0.0042 ± 0.0072 (stat)
Fiducial phase space	-0.0035 ± 0.0072 (stat) ± 0.0031 (syst)
Theoretical prediction [Bernreuther, Si] [11,49]	0.0101 ± 0.0010
Full phase space	0.0010 ± 0.0068 (stat) ± 0.0037 (syst)
Theoretical prediction [Kühn, Rodrigo] [10]	0.0102 ± 0.0005
Theoretical prediction [Bernreuther, Si] [11,49]	0.0111 ± 0.0004

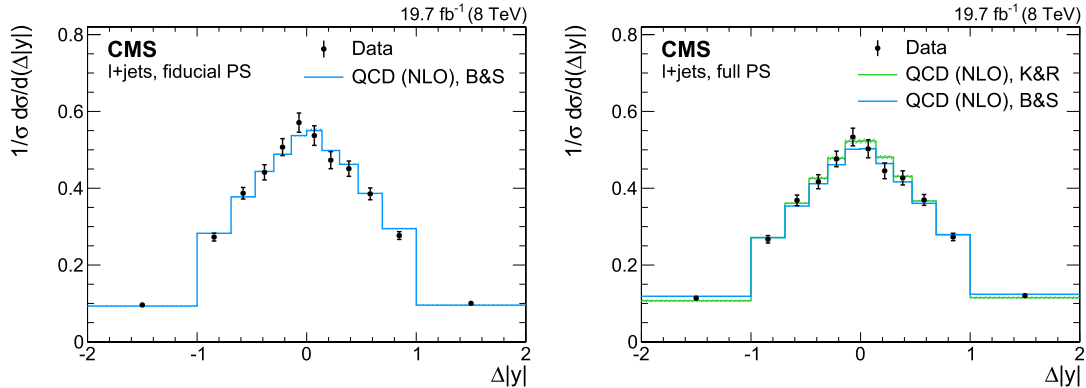


Fig. 3. Unfolded inclusive $\Delta|y|$ distribution in the fiducial phase space (left) and in the full phase space (right). The uncertainties on the data points represent the statistical uncertainties due to the limited amounts of data and simulated events. The measured values are compared to NLO predictions for the SM based on calculations by Kühn and Rodrigo (K&R) [10] and Bernreuther and Si (B&S) [11,49].

The latter two distributions are shown in the form of normalized differential cross sections as a function of $\Delta|y|$. All unfolded quantities correspond to the parton level. The statistical uncertainty of all quoted results encompasses the subdominant effects of the limited number of simulated events used for the measurement. It should be noted that the acceptance corrections for the two phase spaces differ as a function of $\Delta|y|$; as a result, statistical fluctuations in the data can have different effects on the measured asymmetries.

The uncertainty in the theoretical prediction by Kühn and Rodrigo [10] is estimated by varying the top quark mass, the PDFs,

and the μ_R and μ_F scales, with the scale uncertainties being the dominant effect. The uncertainty in the theoretical prediction by Bernreuther and Si [11,49] contains only the effects of variations of the μ_R and μ_F scales. The $t\bar{t}$ charge asymmetry for the fiducial phase space is computed with the $t\bar{t}$ production and semileptonic/non-leptonic $t\bar{t}$ decay matrix elements at NLO. The top quark decay matrix elements at NLO contain additional scale dependencies. This results in a larger scale uncertainty as compared to the charge asymmetry for the full phase space. Another recent CMS analysis of the inclusive charge asymmetry in the full phase space [50], which uses a slightly more model-dependent ap-

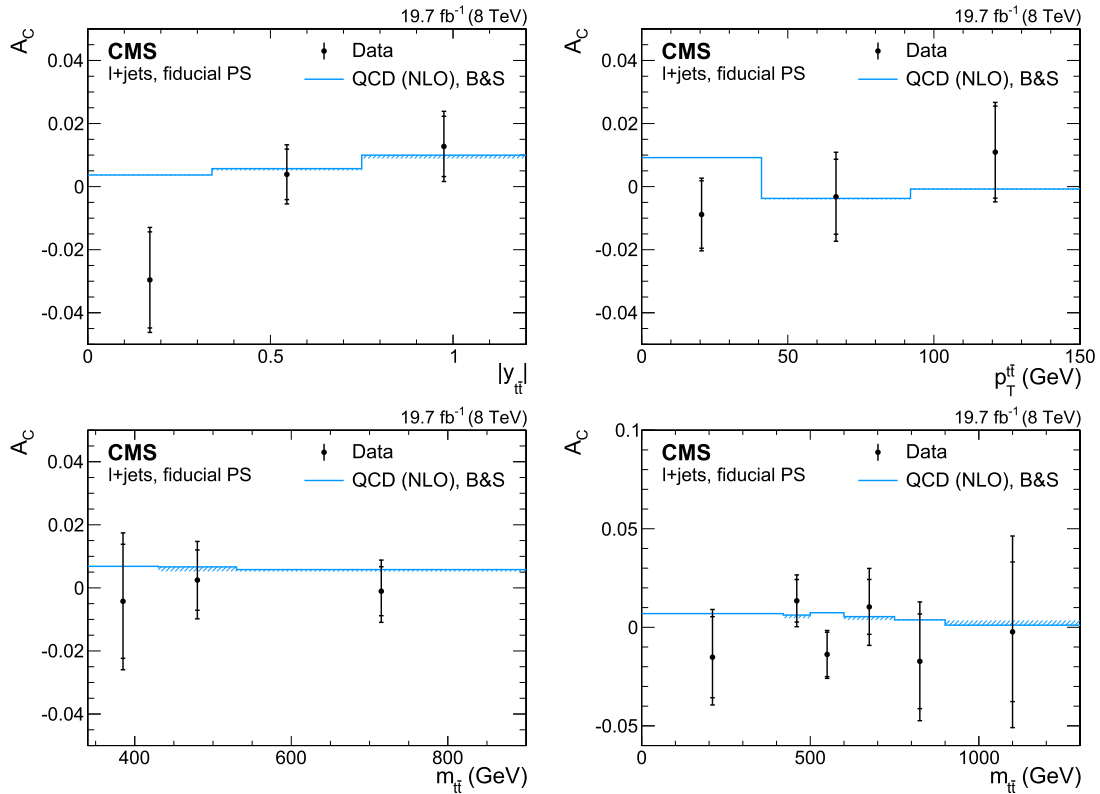


Fig. 4. Corrected asymmetry as a function of $|y_{t\bar{t}}|$ (upper left), $p_T^{t\bar{t}}$ (upper right), and $m_{t\bar{t}}$ (lower left and lower right). The latter is shown in two different binnings. All results correspond to the *fiducial phase space*. The measured values are compared to an NLO prediction for the SM based on calculations by Bernreuther and Si (B&S) [11,49]. The inner bars indicate the statistical uncertainties, while the outer bars represent the statistical and systematic uncertainties added in quadrature.

proach to achieve lower uncertainties, and a recently published ATLAS measurement of inclusive and differential charge asymmetries [51] both yield results that are comparable to the ones presented here.

The results of the differential measurements in the fiducial phase space are shown in Fig. 4, and the extrapolation to the full phase space in Fig. 5. The measured values are compared to predictions from SM calculations [10,11,49] as well as to predictions from an effective field theory [52,53]. The latter is capable of reproducing the CDF results [2] by introducing an anomalous effective axial-vector coupling to the gluon at the one-loop level. The gluon–quark vertex is treated in the approximation of an effective field theory with a scale for new physics contributions of order 1.5–2.0 TeV. Predictions for the asymmetry as a function of $p_T^{t\bar{t}}$ are not available for this theory and for one of the SM calculations. Because of the importance of the region of high $m_{t\bar{t}}$ for the detection of new physics, we provide an additional, more finely-grained differential measurement of the asymmetry as a function of this observable.

Both of the inclusive results yield values that are slightly smaller than the SM predictions, with the larger deviation being in the fiducial phase space and corresponding to 1.7 standard deviations. The differential measurements show a good agreement with the SM predictions. For the benchmark model involving an effective axial-vector coupling of the gluon, the measurement at high $m_{t\bar{t}}$ excludes new physics scales below 1.5 TeV at the 95% confidence level.

10. Summary

Inclusive and differential measurements of the charge asymmetry in $t\bar{t}$ production at the LHC are presented. The data sample,

collected in proton–proton collisions at $\sqrt{s} = 8$ TeV with the CMS detector, corresponds to an integrated luminosity of 19.7 fb^{-1} . Events with top quark pairs decaying into the electron+jets and muon+jets channels are selected and a full $t\bar{t}$ event reconstruction is performed to determine the four-momenta of the top quarks and antiquarks. The observed distributions are then corrected for acceptance and reconstruction effects. For the first time at the LHC, acceptance corrections to the $t\bar{t}$ charge asymmetry are performed not only to the full phase space but also to a fiducial phase space. Within two standard deviations, all measured values are consistent with the predictions of the standard model and no hint of new physics contributions is observed. The charge asymmetry in the high-mass region is about two standard deviations below the predictions from an effective field theory with the scale for new physics at 1.5 TeV.

Acknowledgements

We thank Werner Bernreuther, Zong-Guo Si, Johann Kühn, German Rodrigo, Emidio Gabrielli, Antonio Racioppi, and Martti Raidal for kindly providing theoretical predictions for the differential distributions that are measured in this letter.

We congratulate our colleagues in the CERN accelerator departments for the excellent performance of the LHC and thank the technical and administrative staffs at CERN and at other CMS institutes for their contributions to the success of the CMS effort. In addition, we gratefully acknowledge the computing centres and personnel of the Worldwide LHC Computing Grid for delivering so effectively the computing infrastructure essential to our analyses. Finally, we acknowledge the enduring support for the construction and operation of the LHC and the CMS detector provided by the following funding agencies: BMWFW and FWF (Austria); FNRS

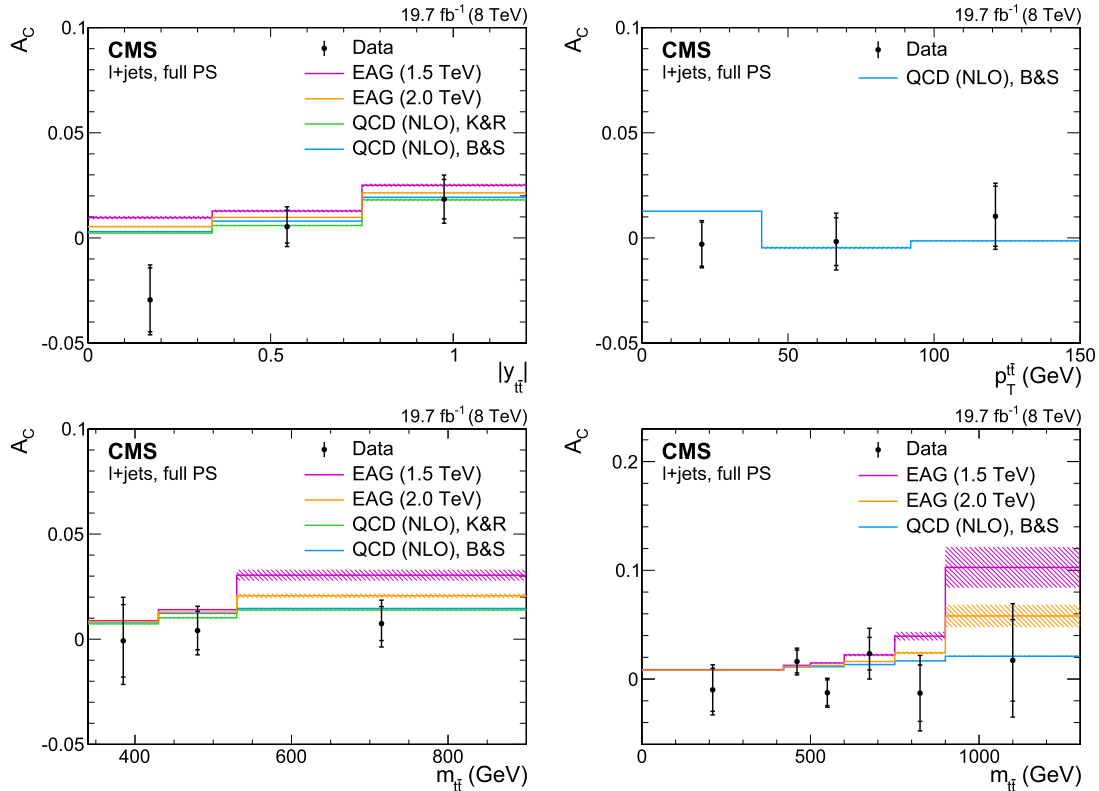


Fig. 5. Corrected asymmetry as a function of $|y_{t\bar{t}}|$ (upper left), $p_T^{t\bar{t}}$ (upper right), and $m_{t\bar{t}}$ (lower left and lower right). The latter is shown in two different binnings. All results correspond to the *full phase space*. The measured values are compared to NLO predictions for the SM based on calculations by Kühn and Rodrigo (K&R) [10] and Bernreuther and Si (B&S) [11,49], as well as to the predictions of a model featuring an effective axial-vector coupling of the gluon (EAG) [52,53]. The inner bars indicate the statistical uncertainties, while the outer bars represent the statistical and systematic uncertainties added in quadrature.

and FWO (Belgium); CNPq, CAPES, FAPERJ, and FAPESP (Brazil); MES (Bulgaria); CERN; CAS, MoST, and NSFC (China); COLCIENCIAS (Colombia); MSES and CSF (Croatia); RPF (Cyprus); MoER, ERC IUT and ERDF (Estonia); Academy of Finland, MEC, and HIP (Finland); CEA and CNRS/IN2P3 (France); BMBF, DFG, and HGF (Germany); GSRT (Greece); OTKA and NIH (Hungary); DAE and DST (India); IPM (Iran); SFI (Ireland); INFN (Italy); MSIP and NRF (Republic of Korea); LAS (Lithuania); MOE and UM (Malaysia); CINVESTAV, CONACYT, SEP, and UASLP-FAI (Mexico); MBIE (New Zealand); PAEC (Pakistan); MSHE and NSC (Poland); FCT (Portugal); JINR (Dubna); MON, RosAtom, RAS and RFBR (Russia); MESTD (Serbia); SEIDI and CPAN (Spain); Swiss Funding Agencies (Switzerland); MST (Taipei); ThEPCenter, IPST, STAR and NSTDA (Thailand); TUBITAK and TAEK (Turkey); NASU and SFFR (Ukraine); STFC (United Kingdom); DOE and NSF (USA).

Individuals have received support from the Marie-Curie programme and the European Research Council and EPLANET (European Union); the Leventis Foundation; the A.P. Sloan Foundation; the Alexander von Humboldt Foundation; the Belgian Federal Science Policy Office; the Fonds pour la Formation à la Recherche dans l'Industrie et dans l'Agriculture (FRIA-Belgium); the Agentschap voor Innovatie door Wetenschap en Technologie (IWT-Belgium); the Ministry of Education, Youth and Sports (MEYS) of the Czech Republic; the Council of Science and Industrial Research, India; the HOMING PLUS programme of the Foundation for Polish Science, cofinanced from European Union, Regional Development Fund; the Compagnia di San Paolo (Torino); the Consorzio per la Fisica (Trieste); MIUR project 20108T4XTM (Italy); the Thalis and Aristeia programmes cofinanced by EU-ESF and the Greek NSRF; the National Priorities Research Program by Qatar National Research Fund; the Rachadapisek Sompot Fund for Postdoctoral Fel-

lowship, Chulalongkorn University (Thailand); and the Welch Foundation.

References

- [1] T. Aaltonen, et al., CDF Collaboration, Evidence for a mass dependent forward-backward asymmetry in top quark pair production, *Phys. Rev. D* 83 (2011) 112003, <http://dx.doi.org/10.1103/PhysRevD.83.112003>.
- [2] T. Aaltonen, et al., CDF Collaboration, Measurement of the top quark forward-backward production asymmetry and its dependence on event kinematic properties, *Phys. Rev. D* 87 (2013) 092002, <http://dx.doi.org/10.1103/PhysRevD.87.092002>, arXiv:1211.1003.
- [3] V.M. Abazov, et al., D0 Collaboration, Forward-backward asymmetry in top quark-antiquark production, *Phys. Rev. D* 84 (2011) 112005, <http://dx.doi.org/10.1103/PhysRevD.84.112005>.
- [4] V.M. Abazov, et al., D0 Collaboration, Measurement of the forward-backward asymmetry in top quark-antiquark production in $p\bar{p}$ collisions using the lepton+jets channel, *Phys. Rev. D* 90 (2014) 072011, <http://dx.doi.org/10.1103/PhysRevD.90.072011>, arXiv:1405.0421.
- [5] V.M. Abazov, et al., D0 Collaboration, Simultaneous measurement of forward-backward asymmetry and top polarization in dilepton final states from $t\bar{t}$ production at the Tevatron, *Phys. Rev. D* 92 (2015) 052007, <http://dx.doi.org/10.1103/PhysRevD.92.052007>.
- [6] M. Czakon, P. Fiedler, A. Mitov, Resolving the Tevatron top quark forward-backward asymmetry puzzle: fully differential next-to-next-to-leading-order calculation, *Phys. Rev. Lett.* 115 (2015) 052001, <http://dx.doi.org/10.1103/PhysRevLett.115.052001>, arXiv:1411.3007.
- [7] N. Kidonakis, The top quark forward-backward asymmetry at approximate N^3 LO, *Phys. Rev. D* 91 (2015) 071502, <http://dx.doi.org/10.1103/PhysRevD.91.071502>, arXiv:1501.01581.
- [8] J.A. Aguilar-Saavedra, D. Amidei, A. Juste, M. Pérez-Victoria, Asymmetries in top quark pair production at hadron colliders, *Rev. Mod. Phys.* 87 (2015) 421, <http://dx.doi.org/10.1103/RevModPhys.87.421>.
- [9] J.H. Kühn, G. Rodrigo, Charge asymmetry in hadroproduction of heavy quarks, *Phys. Rev. Lett.* 81 (1998) 49, <http://dx.doi.org/10.1103/PhysRevLett.81.49>, arXiv: hep-ph/9802268.

- [10] J.H. Kühn, G. Rodrigo, Charge asymmetries of top quarks at hadron colliders revisited, *J. High Energy Phys.* 01 (2012) 063, [http://dx.doi.org/10.1007/JHEP01\(2012\)063](http://dx.doi.org/10.1007/JHEP01(2012)063), arXiv:1109.6830.
- [11] W. Bernreuther, Z.-G. Si, Top quark and leptonic charge asymmetries for the Tevatron and LHC, *Phys. Rev. D* 86 (2012) 034026, <http://dx.doi.org/10.1103/PhysRevD.86.034026>, arXiv:1205.6580.
- [12] CMS Collaboration, Inclusive and differential measurements of the $t\bar{t}$ charge asymmetry in proton–proton collisions at 7 TeV, *Phys. Lett. B* 717 (2012) 129, <http://dx.doi.org/10.1016/j.physletb.2012.09.028>, arXiv:1207.0065.
- [13] ATLAS Collaboration, Measurement of the top quark pair production charge asymmetry in proton–proton collisions at $\sqrt{s} = 7$ TeV using the ATLAS detector, *J. High Energy Phys.* 02 (2014) 107, [http://dx.doi.org/10.1007/JHEP02\(2014\)107](http://dx.doi.org/10.1007/JHEP02(2014)107), arXiv:1311.6724.
- [14] CMS Collaboration, Measurements of the $t\bar{t}$ charge asymmetry using the dilepton decay channel in pp collisions at $\sqrt{s} = 7$ TeV, *J. High Energy Phys.* 04 (2014) 191, [http://dx.doi.org/10.1007/JHEP04\(2014\)191](http://dx.doi.org/10.1007/JHEP04(2014)191), arXiv:1402.3803.
- [15] ATLAS Collaboration, Measurement of the charge asymmetry in dileptonic decays of top quark pairs in pp collisions at $\sqrt{s} = 7$ TeV using the ATLAS detector, *J. High Energy Phys.* 05 (2015) 061, [http://dx.doi.org/10.1007/JHEP05\(2015\)061](http://dx.doi.org/10.1007/JHEP05(2015)061), arXiv:1501.07383.
- [16] G. Rodrigo, P. Ferrario, Charge asymmetry: a theory appraisal, *Nuovo Cimento C* 33 (2010) 221, <http://dx.doi.org/10.1393/ncc/i2010-10646-5>, arXiv:1007.4328.
- [17] CMS Collaboration, Performance of CMS muon reconstruction in pp collision events at $\sqrt{s} = 7$ TeV, *J. Instrum.* 7 (2012) P10002, <http://dx.doi.org/10.1088/1748-0221/7/10/P10002>, arXiv:1206.4071.
- [18] CMS Collaboration, The CMS experiment at the CERN LHC, *J. Instrum.* 3 (2008) S08004, <http://dx.doi.org/10.1088/1748-0221/3/08/S08004>.
- [19] S. Alioli, P. Nason, C. Oleari, E. Re, A general framework for implementing NLO calculations in shower Monte Carlo programs: the POWHEG BOX, *J. High Energy Phys.* 06 (2010) 043, [http://dx.doi.org/10.1007/JHEP06\(2010\)043](http://dx.doi.org/10.1007/JHEP06(2010)043), arXiv:1002.2581.
- [20] P. Nason, A new method for combining NLO QCD with shower Monte Carlo algorithms, *J. High Energy Phys.* 11 (2004) 040, <http://dx.doi.org/10.1088/1126-6708/2004/11/040>, arXiv:hep-ph/0409146.
- [21] S. Frixione, P. Nason, C. Oleari, Matching NLO QCD computations with parton shower simulations: the POWHEG method, *J. High Energy Phys.* 11 (2007) 070, <http://dx.doi.org/10.1088/1126-6708/2007/11/070>, arXiv:0709.2092.
- [22] E. Re, Single-top W t -channel production matched with parton showers using the POWHEG method, *Eur. Phys. J. C* 71 (2011) 1547, <http://dx.doi.org/10.1140/epjc/s10052-011-1547-z>, arXiv:1009.2450.
- [23] H.-L. Lai, M. Guzzi, J. Huston, Z. Li, P.M. Nadolsky, J. Pumplin, C.-P. Yuan, New parton distributions for collider physics, *Phys. Rev. D* 82 (2010) 074024, <http://dx.doi.org/10.1103/PhysRevD.82.074024>, arXiv:1007.2241.
- [24] J. Pumplin, D.R. Stump, J. Huston, H.-L. Lai, P. Nadolsky, W.-K. Tung, New generation of parton distributions with uncertainties from global QCD analysis, *J. High Energy Phys.* 07 (2002) 012, <http://dx.doi.org/10.1088/1126-6708/2002/07/012>, arXiv:hep-ph/0201195.
- [25] J. Alwall, R. Frederix, S. Frixione, V. Hirschi, F. Maltoni, O. Mattelaer, H.-S. Shao, T. Stelzer, P. Torielli, M. Zaro, The automated computation of tree-level and next-to-leading order differential cross sections, and their matching to parton shower simulations, *J. High Energy Phys.* 07 (2014) 079, [http://dx.doi.org/10.1007/JHEP07\(2014\)079](http://dx.doi.org/10.1007/JHEP07(2014)079), arXiv:1405.0301.
- [26] T. Sjöstrand, S. Mrenna, P. Skands, PYTHIA 6.4 physics and manual, *J. High Energy Phys.* 05 (2006) 026, <http://dx.doi.org/10.1088/1126-6708/2006/05/026>, arXiv:hep-ph/0603175.
- [27] CMS Collaboration, Measurement of the differential cross section for top quark pair production in pp collisions at $\sqrt{s} = 8$ TeV, *Eur. Phys. J. C* 75 (2015) 542, <http://dx.doi.org/10.1140/epjc/s10052-015-3709-x>, arXiv:1505.04480.
- [28] CMS Collaboration, Particle-flow event reconstruction in CMS and performance for jets, taus, and E_T^{miss} , CMS physics analysis summary CMS-PAS-PFT-09-001, 2009, <http://cdsweb.cern.ch/record/1194487>.
- [29] CMS Collaboration, Commissioning of the particle-flow event reconstruction with the first LHC collisions recorded in the CMS detector, CMS physics analysis summary CMS-PAS-PFT-10-001, 2010, <http://cdsweb.cern.ch/record/1247373>.
- [30] CMS Collaboration, Description and performance of track and primary-vertex reconstruction with the CMS tracker, *J. Instrum.* 9 (2014) P10009, <http://dx.doi.org/10.1088/1748-0221/9/10/P10009>, arXiv:1405.6569.
- [31] CMS Collaboration, Performance of electron reconstruction and selection with the CMS detector in proton–proton collisions at $\sqrt{s} = 8$ TeV, *J. Instrum.* 10 (2015) P06005, <http://dx.doi.org/10.1088/1748-0221/10/06/P06005>, arXiv:1502.02701.
- [32] M. Cacciari, G.P. Salam, G. Soyez, The anti- k_t jet clustering algorithm, *J. High Energy Phys.* 04 (2008) 063, <http://dx.doi.org/10.1088/1126-6708/2008/04/063>, arXiv:0802.1189.
- [33] CMS Collaboration, Determination of jet energy calibration and transverse momentum resolution in CMS, *J. Instrum.* 6 (2011) P11002, <http://dx.doi.org/10.1088/1748-0221/6/11/P11002>, arXiv:1107.4277.
- [34] CMS Collaboration, Identification of b-quark jets with the CMS experiment, *J. Instrum.* 8 (2013) P04013, <http://dx.doi.org/10.1088/1748-0221/8/04/P04013>.
- [35] CMS Collaboration, Performance of b tagging at $\sqrt{s} = 8$ TeV in multijet, $t\bar{t}$ and boosted topology events, CMS physics analysis summary CMS-PAS-BTV-13-001, 2013, <http://cdsweb.cern.ch/record/1581306>.
- [36] CMS Collaboration, Measurement of the t-channel single-top-quark production cross section and of the $|V_{cb}|$ CKM matrix element in pp collisions at $\sqrt{s} = 8$ TeV, *J. High Energy Phys.* 06 (2014) 090, [http://dx.doi.org/10.1007/JHEP06\(2014\)090](http://dx.doi.org/10.1007/JHEP06(2014)090), arXiv:1403.7366.
- [37] CMS Collaboration, Observation of the associated production of a single top quark and a W boson in pp collisions at $\sqrt{s} = 8$ TeV, *Phys. Rev. Lett.* 112 (2014) 231802, <http://dx.doi.org/10.1103/PhysRevLett.112.231802>, arXiv:1401.2942.
- [38] CMS Collaboration, Measurements of jet multiplicity and differential production cross sections of Z+jets events in proton–proton collisions at $\sqrt{s} = 7$ TeV, *Phys. Rev. D* 91 (2015) 052008, <http://dx.doi.org/10.1103/PhysRevD.91.052008>, arXiv:1408.3104.
- [39] CMS Collaboration, Measurement of the production cross sections for a Z boson and one or more b jets in pp collisions at $\sqrt{s} = 7$ TeV, *J. High Energy Phys.* 06 (2014) 120, [http://dx.doi.org/10.1007/JHEP06\(2014\)120](http://dx.doi.org/10.1007/JHEP06(2014)120), arXiv:1402.1521.
- [40] N. Kidonakis, Differential and total cross sections for top pair and single top production, in: *XX Int. Workshop on Deep-Inelastic Scattering and Related Subjects, Bonn, Germany, 2012*, p. 831, arXiv:1205.3453.
- [41] CMS Collaboration, Measurement of the charge asymmetry in top-quark pair production in proton–proton collisions at $\sqrt{s} = 7$ TeV, *Phys. Lett. B* 709 (2012) 28, <http://dx.doi.org/10.1016/j.physletb.2012.01.078>, arXiv:1112.5100.
- [42] V. Blobel, An unfolding method for high energy physics experiments, arXiv:hep-ex/0208022, 2002.
- [43] G. Corcella, I.G. Knowles, G. Marchesini, S. Moretti, K. Odagiri, P. Richardson, M.H. Seymour, B.R. Webber, HERWIG 6: an event generator for hadron emission reactions with interfering gluons (including supersymmetric processes), *J. High Energy Phys.* 01 (2001) 010, <http://dx.doi.org/10.1088/1126-6708/2001/01/010>, arXiv:hep-ph/0011363.
- [44] G. Corcella, I.G. Knowles, G. Marchesini, S. Moretti, K. Odagiri, P. Richardson, M.H. Seymour, B.R. Webber, HERWIG 6.5 release note, arXiv:hep-ph/0210213, 2002.
- [45] S. Frixione, B.R. Webber, Matching NLO QCD computations and parton shower simulations, *J. High Energy Phys.* 06 (2002) 029, <http://dx.doi.org/10.1088/1126-6708/2002/06/029>, arXiv:hep-ph/0204244.
- [46] M.R. Whalley, D. Bourilkov, R.C. Group, The Les Houches Accord PDFs (LHAPDF) and LHAGLUE, arXiv:hep-ph/0508110, 2005.
- [47] A.D. Martin, W.J. Stirling, R.S. Thorne, G. Watt, Parton distributions for the LHC, *Eur. Phys. J. C* 63 (2009) 189, <http://dx.doi.org/10.1140/epjc/s10052-009-1072-5>, arXiv:0901.0002.
- [48] R.D. Ball, V. Bertone, F. Cerutti, L. Del Debbio, S. Forte, A. Guffanti, J.I. Latorre, J. Rojo, M. Ubiali, NNPDF Collaboration, Impact of heavy quark masses on parton distributions and LHC phenomenology, *Nucl. Phys. B* 849 (2011) 296, <http://dx.doi.org/10.1016/j.nuclphysb.2011.03.021>, arXiv:1101.1300.
- [49] W. Bernreuther, Z.-G. Si, Distributions and correlations for top quark pair production and decay at the Tevatron and LHC, *Nucl. Phys. B* 837 (2010) 90, <http://dx.doi.org/10.1016/j.nuclphysb.2010.05.001>, arXiv:1003.3926.
- [50] CMS Collaboration, Measurement of the charge asymmetry in top quark pair production in pp collisions at $\sqrt{s} = 8$ TeV using a template method, *Phys. Rev. D* 93 (2015) 034014, <http://dx.doi.org/10.1103/PhysRevD.93.034014>, arXiv:1508.03862.
- [51] ATLAS Collaboration, Measurement of the charge asymmetry in top-quark pair production in the lepton-plus-jets final state in pp collision data at $\sqrt{s} = 8$ TeV with the ATLAS detector, *Eur. Phys. J. C* 76 (2016) 87, <http://dx.doi.org/10.1140/epjc/s10052-016-3910-6>, arXiv:1509.02358.
- [52] E. Gabrielli, M. Raidal, A. Racioppi, Implications of the effective axial-vector coupling of gluon on top-quark charge asymmetry at the LHC, *Phys. Rev. D* 85 (2012) 074021, <http://dx.doi.org/10.1103/PhysRevD.85.074021>, arXiv:1112.5885.
- [53] E. Gabrielli, M. Raidal, Effective axial-vector coupling of gluon as an explanation to the top quark asymmetry, *Phys. Rev. D* 84 (2011) 054017, <http://dx.doi.org/10.1103/PhysRevD.84.054017>, arXiv:1106.4553.

CMS Collaboration

V. Khachatryan, A.M. Sirunyan, A. Tumasyan

Yerevan Physics Institute, Yerevan, Armenia

W. Adam, E. Asilar, T. Bergauer, J. Brandstetter, E. Brondolin, M. Dragicevic, J. Erö, M. Flechl, M. Friedl, R. Frühwirth¹, V.M. Ghete, C. Hartl, N. Hörmann, J. Hrubec, M. Jeitler¹, V. Knünz, A. König, M. Krammer¹, I. Krätschmer, D. Liko, T. Matsushita, I. Mikulec, D. Rabady², B. Rahbaran, H. Rohringer, J. Schieck¹, R. Schöfbeck, J. Strauss, W. Treberer-Treberspurg, W. Waltenberger, C.-E. Wulz¹

Institut für Hochenergiephysik der OeAW, Wien, Austria

V. Mossolov, N. Shumeiko, J. Suarez Gonzalez

National Centre for Particle and High Energy Physics, Minsk, Belarus

S. Alderweireldt, T. Cornelis, E.A. De Wolf, X. Janssen, A. Knutsson, J. Lauwers, S. Luyckx, S. Ochesanu, R. Rougny, M. Van De Klundert, H. Van Haevermaet, P. Van Mechelen, N. Van Remortel, A. Van Spilbeeck

Universiteit Antwerpen, Antwerpen, Belgium

S. Abu Zeid, F. Blekman, J. D'Hondt, N. Daci, I. De Bruyn, K. Deroover, N. Heracleous, J. Keaveney, S. Lowette, L. Moreels, A. Olbrechts, Q. Python, D. Strom, S. Tavernier, W. Van Doninck, P. Van Mulders, G.P. Van Onsem, I. Van Parijs

Vrije Universiteit Brussel, Brussel, Belgium

P. Barria, C. Caillol, B. Clerbaux, G. De Lentdecker, H. Delannoy, G. Fasanella, L. Favart, A.P.R. Gay, A. Grebenyuk, T. Lenzi, A. Léonard, T. Maerschalk, A. Marinov, L. Perniè, A. Randle-conde, T. Reis, T. Seva, C. Vander Velde, P. Vanlaer, R. Yonamine, F. Zenoni, F. Zhang³

Université Libre de Bruxelles, Bruxelles, Belgium

K. Beernaert, L. Benucci, A. Cimmino, S. Crucy, D. Dobur, A. Fagot, G. Garcia, M. Gul, J. Mccartin, A.A. Ocampo Rios, D. Poyraz, D. Ryckbosch, S. Salva, M. Sigamani, N. Strobbe, M. Tytgat, W. Van Driessche, E. Yazgan, N. Zaganidis

Ghent University, Ghent, Belgium

S. Basegmez, C. Beluffi⁴, O. Bondu, S. Brochet, G. Bruno, R. Castello, A. Caudron, L. Ceard, G.G. Da Silva, C. Delaere, D. Favart, L. Forthomme, A. Giammanco⁵, J. Hollar, A. Jafari, P. Jez, M. Komm, V. Lemaître, A. Mertens, C. Nuttens, L. Perrini, A. Pin, K. Piotrkowski, A. Popov⁶, L. Quertenmont, M. Selvaggi, M. Vidal Marono

Université Catholique de Louvain, Louvain-la-Neuve, Belgium

N. Beliy, G.H. Hammad

Université de Mons, Mons, Belgium

W.L. Aldá Júnior, G.A. Alves, L. Brito, M. Correa Martins Junior, M. Hamer, C. Hensel, C. Mora Herrera, A. Moraes, M.E. Pol, P. Rebello Teles

Centro Brasileiro de Pesquisas Físicas, Rio de Janeiro, Brazil

E. Belchior Batista Das Chagas, W. Carvalho, J. Chinellato⁷, A. Custódio, E.M. Da Costa, D. De Jesus Damiao, C. De Oliveira Martins, S. Fonseca De Souza, L.M. Huertas Guativa, H. Malbouisson, D. Matos Figueiredo, L. Mundim, H. Nogima, W.L. Prado Da Silva, A. Santoro, A. Sznajder, E.J. Tonelli Manganote⁷, A. Vilela Pereira

Universidade do Estado do Rio de Janeiro, Rio de Janeiro, Brazil

S. Ahuja^a, C.A. Bernardes^b, A. De Souza Santos^b, S. Dogra^a, T.R. Fernandez Perez Tomei^a, E.M. Gregores^b, P.G. Mercadante^b, C.S. Moon^{a,8}, S.F. Novaes^a, Sandra S. Padula^a, D. Romero Abad, J.C. Ruiz Vargas

^a Universidade Estadual Paulista, São Paulo, Brazil

^b Universidade Federal do ABC, São Paulo, Brazil

A. Aleksandrov, V. Genchev[†], R. Hadjiiska, P. Iaydjiev, S. Piperov, M. Rodozov, S. Stoykova, G. Sultanov, M. Vutova

Institute for Nuclear Research and Nuclear Energy, Sofia, Bulgaria

A. Dimitrov, I. Glushkov, L. Litov, B. Pavlov, P. Petkov

University of Sofia, Sofia, Bulgaria

M. Ahmad, J.G. Bian, G.M. Chen, H.S. Chen, M. Chen, T. Cheng, R. Du, C.H. Jiang, R. Plestina⁹, F. Romeo, S.M. Shaheen, J. Tao, C. Wang, Z. Wang, H. Zhang

Institute of High Energy Physics, Beijing, China

C. Asawatangtrakuldee, Y. Ban, Q. Li, S. Liu, Y. Mao, S.J. Qian, D. Wang, Z. Xu, W. Zou

State Key Laboratory of Nuclear Physics and Technology, Peking University, Beijing, China

C. Avila, A. Cabrera, L.F. Chaparro Sierra, C. Florez, J.P. Gomez, B. Gomez Moreno, J.C. Sanabria

Universidad de Los Andes, Bogota, Colombia

N. Godinovic, D. Lelas, D. Polic, I. Puljak, P.M. Ribeiro Cipriano

University of Split, Faculty of Electrical Engineering, Mechanical Engineering and Naval Architecture, Split, Croatia

Z. Antunovic, M. Kovac

University of Split, Faculty of Science, Split, Croatia

V. Brigljevic, K. Kadija, J. Luetic, S. Micanovic, L. Sudic

Institute Rudjer Boskovic, Zagreb, Croatia

A. Attikis, G. Mavromanolakis, J. Mousa, C. Nicolaou, F. Ptochos, P.A. Razis, H. Rykaczewski

University of Cyprus, Nicosia, Cyprus

M. Bodlak, M. Finger¹⁰, M. Finger Jr.¹⁰

Charles University, Prague, Czech Republic

A.A. Abdelalim¹¹, A. Awad^{12,13}, A. Mahrous¹⁴, A. Radi^{13,12}

Academy of Scientific Research and Technology of the Arab Republic of Egypt, Egyptian Network of High Energy Physics, Cairo, Egypt

B. Calpas, M. Kadastik, M. Murumaa, M. Raidal, A. Tiko, C. Veelken

National Institute of Chemical Physics and Biophysics, Tallinn, Estonia

P. Eerola, J. Pekkanen, M. Voutilainen

Department of Physics, University of Helsinki, Helsinki, Finland

J. Härkönen, V. Karimäki, R. Kinnunen, T. Lampén, K. Lassila-Perini, S. Lehti, T. Lindén, P. Luukka, T. Mäenpää, T. Peltola, E. Tuominen, J. Tuominiemi, E. Tuovinen, L. Wendland

Helsinki Institute of Physics, Helsinki, Finland

J. Talvitie, T. Tuuva

Lappeenranta University of Technology, Lappeenranta, Finland

M. Besancon, F. Couderc, M. Dejardin, D. Denegri, B. Fabbro, J.L. Faure, C. Favaro, F. Ferri, S. Ganjour, A. Givernaud, P. Gras, G. Hamel de Monchenault, P. Jarry, E. Locci, M. Machet, J. Malcles, J. Rander, A. Rosowsky, M. Titov, A. Zghiche

DSM/IRFU, CEA/Saclay, Gif-sur-Yvette, France

I. Antropov, S. Baffioni, F. Beaudette, P. Busson, L. Cadamuro, E. Chapon, C. Charlot, T. Dahms, O. Davignon, N. Filipovic, A. Florent, R. Granier de Cassagnac, S. Lisniak, L. Mastrolorenzo, P. Miné, I.N. Naranjo, M. Nguyen, C. Ochando, G. Ortona, P. Paganini, S. Regnard, R. Salerno, J.B. Sauvan, Y. Sirois, T. Strebler, Y. Yilmaz, A. Zabi

Laboratoire Leprince-Ringuet, Ecole Polytechnique, IN2P3–CNRS, Palaiseau, France

J.-L. Agram¹⁵, J. Andrea, A. Aubin, D. Bloch, J.-M. Brom, M. Buttignol, E.C. Chabert, N. Chanon, C. Collard, E. Conte¹⁵, X. Coubez, J.-C. Fontaine¹⁵, D. Gelé, U. Goerlach, C. Goetzmann, A.-C. Le Bihan, J.A. Merlin², K. Skovpen, P. Van Hove

Institut Pluridisciplinaire Hubert Curien, Université de Strasbourg, Université de Haute Alsace Mulhouse, CNRS/IN2P3, Strasbourg, France

S. Gadrat

Centre de Calcul de l'Institut National de Physique Nucleaire et de Physique des Particules, CNRS/IN2P3, Villeurbanne, France

S. Beauceron, C. Bernet, G. Boudoul, E. Bouvier, C.A. Carrillo Montoya, J. Chasserat, R. Chierici, D. Contardo, B. Courbon, P. Depasse, H. El Mamouni, J. Fan, J. Fay, S. Gascon, M. Gouzevitch, B. Ille, F. Lagarde, I.B. Laktineh, M. Lethuillier, L. Mirabito, A.L. Pequegnot, S. Perries, J.D. Ruiz Alvarez, D. Sabes, L. Sgandurra, V. Sordini, M. Vander Donckt, P. Verdier, S. Viret, H. Xiao

Université de Lyon, Université Claude Bernard Lyon 1, CNRS–IN2P3, Institut de Physique Nucléaire de Lyon, Villeurbanne, France

T. Toriashvili¹⁶

Georgian Technical University, Tbilisi, Georgia

I. Bagaturia¹⁷

Tbilisi State University, Tbilisi, Georgia

C. Autermann, S. Beranek, M. Edelhoff, L. Feld, A. Heister, M.K. Kiesel, K. Klein, M. Lipinski, A. Ostapchuk, M. Preuten, F. Raupach, S. Schael, J.F. Schulte, T. Verlage, H. Weber, B. Wittmer, V. Zhukov⁶

RWTH Aachen University, I. Physikalisches Institut, Aachen, Germany

M. Ata, M. Brodski, E. Dietz-Laursonn, D. Duchardt, M. Endres, M. Erdmann, S. Erdweg, T. Esch, R. Fischer, A. Güth, T. Hebbeker, C. Heidemann, K. Hoepfner, D. Klingebiel, S. Knutzen, P. Kreuzer, M. Merschmeyer, A. Meyer, P. Millet, M. Olschewski, K. Padeken, P. Papacz, T. Pook, M. Radziej, H. Reithler, M. Rieger, F. Scheuch, L. Sonnenschein, D. Teyssier, S. Thüer

RWTH Aachen University, III. Physikalisches Institut A, Aachen, Germany

V. Cherepanov, Y. Erdogan, G. Flügge, H. Geenen, M. Geisler, F. Hoehle, B. Kargoll, T. Kress, Y. Kuessel, A. Künsken, J. Lingemann², A. Nehr Korn, A. Nowack, I.M. Nugent, C. Pistone, O. Pooth, A. Stahl

RWTH Aachen University, III. Physikalisches Institut B, Aachen, Germany

M. Aldaya Martin, I. Asin, N. Bartosik, O. Behnke, U. Behrens, A.J. Bell, K. Borras, A. Burgmeier, A. Cakir, L. Calligaris, A. Campbell, S. Choudhury, F. Costanza, C. Diez Pardos, G. Dolinska, S. Dooling, T. Dorland, G. Eckerlin, D. Eckstein, T. Eichhorn, G. Flucke, E. Gallo, J. Garay Garcia, A. Geiser, A. Gizhko,

P. Gunnellini, J. Hauk, M. Hempel¹⁸, H. Jung, A. Kalogeropoulos, O. Karacheban¹⁸, M. Kasemann, P. Katsas, J. Kieseler, C. Kleinwort, I. Korol, W. Lange, J. Leonard, K. Lipka, A. Lobanov, W. Lohmann¹⁸, R. Mankel, I. Marfin¹⁸, I.-A. Melzer-Pellmann, A.B. Meyer, G. Mittag, J. Mnich, A. Mussgiller, S. Naumann-Emme, A. Nayak, E. Ntomari, H. Perrey, D. Pitzl, R. Placakyte, A. Raspereza, B. Roland, M.Ö. Sahin, P. Saxena, T. Schoerner-Sadenius, M. Schröder, C. Seitz, S. Spannagel, K.D. Trippkewitz, C. Wissing

Deutsches Elektronen-Synchrotron, Hamburg, Germany

V. Blobel, M. Centis Vignali, A.R. Draeger, J. Erfle, E. Garutti, K. Goebel, D. Gonzalez, M. Görner, J. Haller, M. Hoffmann, R.S. Höing, A. Junkes, R. Klanner, R. Kogler, T. Lapsien, T. Lenz, I. Marchesini, D. Marconi, D. Nowatschin, J. Ott, F. Pantaleo², T. Peiffer, A. Perieanu, N. Pietsch, J. Poehlsen, D. Rathjens, C. Sander, H. Schettler, P. Schleper, E. Schlieckau, A. Schmidt, J. Schwandt, M. Seidel, V. Sola, H. Stadie, G. Steinbrück, H. Tholen, D. Troendle, E. Usai, L. Vanelderren, A. Vanhoefer

University of Hamburg, Hamburg, Germany

M. Akbiyik, C. Barth, C. Baus, J. Berger, C. Böser, E. Butz, T. Chwalek, F. Colombo, W. De Boer, A. Descroix, A. Dierlamm, S. Fink, F. Frensch, M. Giffels, A. Gilbert, F. Hartmann², S.M. Heindl, U. Husemann, I. Katkov⁶, A. Kornmayer², P. Lobelle Pardo, B. Maier, H. Mildner, M.U. Mozer, T. Müller, Th. Müller, M. Plagge, G. Quast, K. Rabbertz, S. Röcker, F. Roscher, H.J. Simonis, F.M. Stober, R. Ulrich, J. Wagner-Kuhr, S. Wayand, M. Weber, T. Weiler, C. Wöhrmann, R. Wolf

Institut für Experimentelle Kernphysik, Karlsruhe, Germany

G. Anagnostou, G. Daskalakis, T. Geralis, V.A. Giakoumopoulou, A. Kyriakis, D. Loukas, A. Psallidas, I. Topsis-Giotis

Institute of Nuclear and Particle Physics (INPP), NCSR Demokritos, Aghia Paraskevi, Greece

A. Agapitos, S. Kesisoglou, A. Panagiotou, N. Saoulidou, E. Tziaferi

University of Athens, Athens, Greece

I. Evangelou, G. Flouris, C. Foudas, P. Kokkas, N. Loukas, N. Manthos, I. Papadopoulos, E. Paradas, J. Strologas

University of Ioánnina, Ioánnina, Greece

G. Bencze, C. Hajdu, A. Hazi, P. Hidas, D. Horvath¹⁹, F. Sikler, V. Veszpremi, G. Vesztergombi²⁰, A.J. Zsigmond

Wigner Research Centre for Physics, Budapest, Hungary

N. Beni, S. Czellar, J. Karancsi²¹, J. Molnar, Z. Szillasi

Institute of Nuclear Research ATOMKI, Debrecen, Hungary

M. Bartók²², A. Makovec, P. Raics, Z.L. Trocsanyi, B. Ujvari

University of Debrecen, Debrecen, Hungary

P. Mal, K. Mandal, N. Sahoo, S.K. Swain

National Institute of Science Education and Research, Bhubaneswar, India

S. Bansal, S.B. Beri, V. Bhatnagar, R. Chawla, R. Gupta, U. Bhawandeep, A.K. Kalsi, A. Kaur, M. Kaur, R. Kumar, A. Mehta, M. Mittal, J.B. Singh, G. Walia

Panjab University, Chandigarh, India

Ashok Kumar, Arun Kumar, A. Bhardwaj, B.C. Choudhary, R.B. Garg, A. Kumar, S. Malhotra, M. Naimuddin, N. Nishu, K. Ranjan, R. Sharma, V. Sharma

University of Delhi, Delhi, India

S. Banerjee, S. Bhattacharya, K. Chatterjee, S. Dey, S. Dutta, Sa. Jain, N. Majumdar, A. Modak, K. Mondal, S. Mukherjee, S. Mukhopadhyay, A. Roy, D. Roy, S. Roy Chowdhury, S. Sarkar, M. Sharan

Saha Institute of Nuclear Physics, Kolkata, India

A. Abdulsalam, R. Chudasama, D. Dutta, V. Jha, V. Kumar, A.K. Mohanty², L.M. Pant, P. Shukla, A. Topkar

Bhabha Atomic Research Centre, Mumbai, India

T. Aziz, S. Banerjee, S. Bhowmik²³, R.M. Chatterjee, R.K. Dewanjee, S. Dugad, S. Ganguly, S. Ghosh, M. Guchait, A. Gurtu²⁴, G. Kole, S. Kumar, B. Mahakud, M. Maity²³, G. Majumder, K. Mazumdar, S. Mitra, G.B. Mohanty, B. Parida, T. Sarkar²³, K. Sudhakar, N. Sur, B. Sutar, N. Wickramage²⁵

Tata Institute of Fundamental Research, Mumbai, India

S. Chauhan, S. Dube, S. Sharma

Indian Institute of Science Education and Research (IISER), Pune, India

H. Bakhshiansohi, H. Behnamian, S.M. Etesami²⁶, A. Fahim²⁷, R. Goldouzian, M. Khakzad, M. Mohammadi Najafabadi, M. Naseri, S. Paktinat Mehdiabadi, F. Rezaei Hosseinabadi, B. Safarzadeh²⁸, M. Zeinali

Institute for Research in Fundamental Sciences (IPM), Tehran, Iran

M. Felcini, M. Grunewald

University College Dublin, Dublin, Ireland

M. Abbrescia^{a,b}, C. Calabria^{a,b}, C. Caputo^{a,b}, S.S. Chhibra^{a,b}, A. Colaleo^a, D. Creanza^{a,c}, L. Cristella^{a,b}, N. De Filippis^{a,c}, M. De Palma^{a,b}, L. Fiore^a, G. Iaselli^{a,c}, G. Maggi^{a,c}, M. Maggi^a, G. Miniello^{a,b}, S. My^{a,c}, S. Nuzzo^{a,b}, A. Pompili^{a,b}, G. Pugliese^{a,c}, R. Radogna^{a,b}, A. Ranieri^a, G. Selvaggi^{a,b}, L. Silvestris^{a,2}, R. Venditti^{a,b}, P. Verwilligen^a

^a INFN Sezione di Bari, Bari, Italy

^b Università di Bari, Bari, Italy

^c Politecnico di Bari, Bari, Italy

G. Abbiendi^a, C. Battilana², A.C. Benvenuti^a, D. Bonacorsi^{a,b}, S. Braibant-Giacomelli^{a,b}, L. Brigliadori^{a,b}, R. Campanini^{a,b}, P. Capiluppi^{a,b}, A. Castro^{a,b}, F.R. Cavallo^a, G. Codispoti^{a,b}, M. Cuffiani^{a,b}, G.M. Dallavalle^a, F. Fabbri^a, A. Fanfani^{a,b}, D. Fasanella^{a,b}, P. Giacomelli^a, C. Grandi^a, L. Guiducci^{a,b}, S. Marcellini^a, G. Masetti^a, A. Montanari^a, F.L. Navarria^{a,b}, A. Perrotta^a, A.M. Rossi^{a,b}, T. Rovelli^{a,b}, G.P. Siroli^{a,b}, N. Tosi^{a,b}, R. Travaglini^{a,b}

^a INFN Sezione di Bologna, Bologna, Italy

^b Università di Bologna, Bologna, Italy

G. Cappello^a, M. Chiorboli^{a,b}, S. Costa^{a,b}, F. Giordano^a, R. Potenza^{a,b}, A. Tricomi^{a,b}, C. Tuve^{a,b}

^a INFN Sezione di Catania, Catania, Italy

^b Università di Catania, Catania, Italy

^c CSFNSM, Catania, Italy

G. Barbagli^a, V. Ciulli^{a,b}, C. Civinini^a, R. D'Alessandro^{a,b}, E. Focardi^{a,b}, S. Gonzi^{a,b}, V. Gori^{a,b}, P. Lenzi^{a,b}, M. Meschini^a, S. Paoletti^a, G. Sguazzoni^a, A. Tropiano^{a,b}, L. Viliani^{a,b}

^a INFN Sezione di Firenze, Firenze, Italy

^b Università di Firenze, Firenze, Italy

L. Benussi, S. Bianco, F. Fabbri, D. Piccolo

INFN Laboratori Nazionali di Frascati, Frascati, Italy

V. Calvelli^{a,b}, F. Ferro^a, M. Lo Vetere^{a,b}, M.R. Monge^{a,b}, E. Robutti^a, S. Tosi^{a,b}

^a INFN Sezione di Genova, Genova, Italy

^b Università di Genova, Genova, Italy

L. Brianza, M.E. Dinardo^{a,b}, S. Fiorendi^{a,b}, S. Gennai^a, R. Gerosa^{a,b}, A. Ghezzi^{a,b}, P. Govoni^{a,b}, S. Malvezzi^a, R.A. Manzoni^{a,b}, B. Marzocchi^{a,b,2}, D. Menasce^a, L. Moroni^a, M. Paganoni^{a,b}, D. Pedrini^a, S. Ragazzi^{a,b}, N. Redaelli^a, T. Tabarelli de Fatis^{a,b}

^a INFN Sezione di Milano-Bicocca, Milano, Italy

^b Università di Milano-Bicocca, Milano, Italy

S. Buontempo^a, N. Cavallo^{a,c}, S. Di Guida^{a,d,2}, M. Esposito^{a,b}, F. Fabozzi^{a,c}, A.O.M. Iorio^{a,b}, G. Lanza^a, L. Lista^a, S. Meola^{a,d,2}, M. Merola^a, P. Paolucci^{a,2}, C. Sciacca^{a,b}, F. Thyssen

^a INFN Sezione di Napoli, Napoli, Italy

^b Università di Napoli 'Federico II', Napoli, Italy

^c Università della Basilicata, Potenza, Italy

^d Università G. Marconi, Roma, Italy

P. Azzi^{a,2}, N. Bacchetta^a, L. Benato^{a,b}, D. Bisello^{a,b}, A. Boletti^{a,b}, R. Carlin^{a,b}, A. Carvalho Antunes De Oliveira^{a,b}, P. Checchia^a, M. Dall'Osso^{a,b,2}, T. Dorigo^a, U. Dosselli^a, F. Gasparini^{a,b}, U. Gasparini^{a,b}, F. Gonella^a, A. Gozzelino^a, M. Gulmini^{a,29}, S. Lacaprara^a, M. Margoni^{a,b}, A.T. Meneguzzo^{a,b}, J. Pazzini^{a,b}, N. Pozzobon^{a,b}, P. Ronchese^{a,b}, F. Simonetto^{a,b}, E. Torassa^a, M. Tosi^{a,b}, M. Zanetti, P. Zotto^{a,b}, A. Zucchetta^{a,b,2}, G. Zumerle^{a,b}

^a INFN Sezione di Padova, Padova, Italy

^b Università di Padova, Padova, Italy

^c Università di Trento, Trento, Italy

A. Braghieri^a, A. Magnani^a, P. Montagna^{a,b}, S.P. Ratti^{a,b}, V. Re^a, C. Riccardi^{a,b}, P. Salvini^a, I. Vai^a, P. Vitulo^{a,b}

^a INFN Sezione di Pavia, Pavia, Italy

^b Università di Pavia, Pavia, Italy

L. Alunni Solestizi^{a,b}, M. Biasini^{a,b}, G.M. Bilei^a, D. Ciangottini^{a,b,2}, L. Fanò^{a,b}, P. Lariccia^{a,b}, G. Mantovani^{a,b}, M. Menichelli^a, A. Saha^a, A. Santocchia^{a,b}, A. Spiezia^{a,b}

^a INFN Sezione di Perugia, Perugia, Italy

^b Università di Perugia, Perugia, Italy

K. Androsov^{a,30}, P. Azzurri^a, G. Bagliesi^a, J. Bernardini^a, T. Boccali^a, G. Broccolo^{a,c}, R. Castaldi^a, M.A. Ciocci^{a,30}, R. Dell'Orso^a, S. Donato^{a,c,2}, G. Fedi, L. Foà^{a,c,†}, A. Giassi^a, M.T. Grippo^{a,30}, F. Ligabue^{a,c}, T. Lomtadze^a, L. Martini^{a,b}, A. Messineo^{a,b}, F. Palla^a, A. Rizzi^{a,b}, A. Savoy-Navarro^{a,31}, A.T. Serban^a, P. Spagnolo^a, P. Squillacioti^{a,30}, R. Tenchini^a, G. Tonelli^{a,b}, A. Venturi^a, P.G. Verdini^a

^a INFN Sezione di Pisa, Pisa, Italy

^b Università di Pisa, Pisa, Italy

^c Scuola Normale Superiore di Pisa, Pisa, Italy

L. Barone^{a,b}, F. Cavallari^a, G. D'imperio^{a,b,2}, D. Del Re^{a,b}, M. Diemoz^a, S. Gelli^{a,b}, C. Jorda^a, E. Longo^{a,b}, F. Margaroli^{a,b}, P. Meridiani^a, F. Micheli^{a,b}, G. Organtini^{a,b}, R. Paramatti^a, F. Preiato^{a,b}, S. Rahatlou^{a,b}, C. Rovelli^a, F. Santanastasio^{a,b}, P. Traczyk^{a,b,2}

^a INFN Sezione di Roma, Roma, Italy

^b Università di Roma, Roma, Italy

N. Amapane^{a,b}, R. Arcidiacono^{a,c,2}, S. Argiro^{a,b}, M. Arneodo^{a,c}, R. Bellan^{a,b}, C. Biino^a, N. Cartiglia^a, M. Costa^{a,b}, R. Covarelli^{a,b}, A. Degano^{a,b}, N. Demaria^a, L. Finco^{a,b,2}, B. Kiani^{a,b}, C. Mariotti^a, S. Maselli^a, E. Migliore^{a,b}, V. Monaco^{a,b}, E. Monteil^{a,b}, M. Musich^a, M.M. Obertino^{a,b}, L. Pacher^{a,b},

N. Pastrone^a, M. Pelliccioni^a, G.L. Pinna Angioni^{a,b}, F. Ravera^{a,b}, A. Romero^{a,b}, M. Ruspa^{a,c}, R. Sacchi^{a,b}, A. Solano^{a,b}, A. Staiano^a, U. Tamponi^a

^a INFN Sezione di Torino, Torino, Italy

^b Università di Torino, Torino, Italy

^c Università del Piemonte Orientale, Novara, Italy

S. Belforte^a, V. Candelise^{a,b,2}, M. Casarsa^a, F. Cossutti^a, G. Della Ricca^{a,b}, B. Gobbo^a, C. La Licata^{a,b}, M. Marone^{a,b}, A. Schizzi^{a,b}, T. Umer^{a,b}, A. Zanetti^a

^a INFN Sezione di Trieste, Trieste, Italy

^b Università di Trieste, Trieste, Italy

S. Chang, A. Kropivnitskaya, S.K. Nam

Kangwon National University, Chunchon, Republic of Korea

D.H. Kim, G.N. Kim, M.S. Kim, D.J. Kong, S. Lee, Y.D. Oh, A. Sakharov, D.C. Son

Kyungpook National University, Daegu, Republic of Korea

J.A. Brochero Cifuentes, H. Kim, T.J. Kim, M.S. Ryu

Chonbuk National University, Jeonju, Republic of Korea

S. Song

Chonnam National University, Institute for Universe and Elementary Particles, Kwangju, Republic of Korea

S. Choi, Y. Go, D. Gyun, B. Hong, M. Jo, H. Kim, Y. Kim, B. Lee, K. Lee, K.S. Lee, S. Lee, S.K. Park, Y. Roh

Korea University, Seoul, Republic of Korea

H.D. Yoo

Seoul National University, Seoul, Republic of Korea

M. Choi, H. Kim, J.H. Kim, J.S.H. Lee, I.C. Park, G. Ryu

University of Seoul, Seoul, Republic of Korea

Y. Choi, Y.K. Choi, J. Goh, D. Kim, E. Kwon, J. Lee, I. Yu

Sungkyunkwan University, Suwon, Republic of Korea

A. Juodagalvis, J. Vaitkus

Vilnius University, Vilnius, Lithuania

I. Ahmed, Z.A. Ibrahim, J.R. Komaragiri, M.A.B. Md Ali³², F. Mohamad Idris³³, W.A.T. Wan Abdullah, M.N. Yusli

National Centre for Particle Physics, Universiti Malaya, Kuala Lumpur, Malaysia

E. Casimiro Linares, H. Castilla-Valdez, E. De La Cruz-Burelo, I. Heredia-de La Cruz³⁴, A. Hernandez-Almada, R. Lopez-Fernandez, A. Sanchez-Hernandez

Centro de Investigacion y de Estudios Avanzados del IPN, Mexico City, Mexico

S. Carrillo Moreno, F. Vazquez Valencia

Universidad Iberoamericana, Mexico City, Mexico

S. Carpinteyro, I. Pedraza, H.A. Salazar Ibarquen

Benemerita Universidad Autonoma de Puebla, Puebla, Mexico

A. Morelos Pineda

Universidad Autónoma de San Luis Potosí, San Luis Potosí, Mexico

D. Krofcheck

University of Auckland, Auckland, New Zealand

P.H. Butler, S. Reucroft

University of Canterbury, Christchurch, New Zealand

A. Ahmad, M. Ahmad, Q. Hassan, H.R. Hoorani, W.A. Khan, T. Khurshid, M. Shoaib

National Centre for Physics, Quaid-I-Azam University, Islamabad, Pakistan

H. Bialkowska, M. Bluj, B. Boimska, T. Frueboes, M. Górski, M. Kazana, K. Nawrocki, K. Romanowska-Rybinska, M. Szleper, P. Zalewski

National Centre for Nuclear Research, Swierk, Poland

G. Brona, K. Bunkowski, K. Doroba, A. Kalinowski, M. Konecki, J. Krolikowski, M. Misiura, M. Olszewski, M. Walczak

Institute of Experimental Physics, Faculty of Physics, University of Warsaw, Warsaw, Poland

P. Bargassa, C. Beirão Da Cruz E Silva, A. Di Francesco, P. Faccioli, P.G. Ferreira Parracho, M. Gallinaro, N. Leonardo, L. Lloret Iglesias, F. Nguyen, J. Rodrigues Antunes, J. Seixas, O. Toldaiev, D. Vadrucio, J. Varela, P. Vischia

Laboratório de Instrumentação e Física Experimental de Partículas, Lisboa, Portugal

S. Afanasiev, P. Bunin, M. Gavrilenko, I. Golutvin, I. Gorbunov, A. Kamenev, V. Karjavin, V. Konoplyanikov, A. Lanev, A. Malakhov, V. Matveev³⁵, P. Moisezenz, V. Palichik, V. Perelygin, S. Shmatov, S. Shulha, N. Skatchkov, V. Smirnov, A. Zarubin

Joint Institute for Nuclear Research, Dubna, Russia

V. Golovtsov, Y. Ivanov, V. Kim³⁶, E. Kuznetsova, P. Levchenko, V. Murzin, V. Oreshkin, I. Smirnov, V. Sulimov, L. Uvarov, S. Vavilov, A. Vorobyev

Petersburg Nuclear Physics Institute, Gatchina (St. Petersburg), Russia

Yu. Andreev, A. Dermenev, S. Gninenko, N. Golubev, A. Karneyeu, M. Kirsanov, N. Krasnikov, A. Pashenkov, D. Tlisov, A. Toropin

Institute for Nuclear Research, Moscow, Russia

V. Epshteyn, V. Gavrillov, N. Lychkovskaya, V. Popov, I. Pozdnyakov, G. Safronov, A. Spiridonov, E. Vlasov, A. Zhokin

Institute for Theoretical and Experimental Physics, Moscow, Russia

A. Bylinkin

National Research Nuclear University 'Moscow Engineering Physics Institute' (MEPhI), Moscow, Russia

V. Andreev, M. Azarkin³⁷, I. Dremin³⁷, M. Kirakosyan, A. Leonidov³⁷, G. Mesyats, S.V. Rusakov, A. Vinogradov

P.N. Lebedev Physical Institute, Moscow, Russia

A. Baskakov, A. Belyaev, E. Boos, V. Bunichev, M. Dubinin³⁸, L. Dudko, A. Ershov, V. Klyukhin, O. Kodolova, N. Korneeva, I. Lokhtin, I. Myagkov, S. Obraztsov, M. Perfilov, V. Savrin

Skobeltsyn Institute of Nuclear Physics, Lomonosov Moscow State University, Moscow, Russia

I. Azhgirey, I. Bayshev, S. Bitioukov, V. Kachanov, A. Kalinin, D. Konstantinov, V. Krychkin, V. Petrov, R. Ryutin, A. Sobol, L. Tourtchanovitch, S. Troshin, N. Tyurin, A. Uzunian, A. Volkov

State Research Center of Russian Federation, Institute for High Energy Physics, Protvino, Russia

P. Adzic³⁹, M. Ekmedzic, J. Milosevic, V. Rekovic

University of Belgrade, Faculty of Physics and Vinca Institute of Nuclear Sciences, Belgrade, Serbia

J. Alcaraz Maestre, E. Calvo, M. Cerrada, M. Chamizo Llatas, N. Colino, B. De La Cruz, A. Delgado Peris, D. Domínguez Vázquez, A. Escalante Del Valle, C. Fernandez Bedoya, J.P. Fernández Ramos, J. Flix, M.C. Fouz, P. Garcia-Abia, O. Gonzalez Lopez, S. Goy Lopez, J.M. Hernandez, M.I. Josa, E. Navarro De Martino, A. Pérez-Calero Yzquierdo, J. Puerta Pelayo, A. Quintario Olmeda, I. Redondo, L. Romero, M.S. Soares

Centro de Investigaciones Energéticas Medioambientales y Tecnológicas (CIEMAT), Madrid, Spain

C. Albajar, J.F. de Trocóniz, M. Missiroli, D. Moran

Universidad Autónoma de Madrid, Madrid, Spain

H. Brun, J. Cuevas, J. Fernandez Menendez, S. Folgueras, I. Gonzalez Caballero, E. Palencia Cortezon, J.M. Vizán García

Universidad de Oviedo, Oviedo, Spain

I.J. Cabrillo, A. Calderon, J.R. Castiñeiras De Saa, P. De Castro Manzano, J. Duarte Campderros, M. Fernandez, G. Gomez, A. Graziano, A. Lopez Virto, J. Marco, R. Marco, C. Martinez Rivero, F. Matorras, F.J. Munoz Sanchez, J. Piedra Gomez, T. Rodrigo, A.Y. Rodríguez-Marrero, A. Ruiz-Jimeno, L. Scodellaro, I. Vila, R. Vilar Cortabitarte

Instituto de Física de Cantabria (IFCA), CSIC– Universidad de Cantabria, Santander, Spain

D. Abbaneo, E. Auffray, G. Auzinger, M. Bachtis, P. Baillon, A.H. Ball, D. Barney, A. Benaglia, J. Bendavid, L. Benhabib, J.F. Benitez, G.M. Berruti, P. Bloch, A. Bocci, A. Bonato, C. Botta, H. Breuker, T. Camporesi, G. Cerminara, S. Colafranceschi⁴⁰, M. D'Alfonso, D. d'Enterria, A. Dabrowski, V. Daponte, A. David, M. De Gruttola, F. De Guio, A. De Roeck, S. De Visscher, E. Di Marco, M. Dobson, M. Dordevic, B. Dorney, T. du Pree, N. Dupont, A. Elliott-Peisert, G. Franzoni, W. Funk, D. Gigi, K. Gill, D. Giordano, M. Girone, F. Glege, R. Guida, S. Gundacker, M. Guthoff, J. Hammer, P. Harris, J. Hegeman, V. Innocente, P. Janot, H. Kirschenmann, M.J. Kortelainen, K. Kousouris, K. Krajczar, P. Lecoq, C. Lourenço, M.T. Lucchini, N. Magini, L. Malgeri, M. Mannelli, A. Martelli, L. Masetti, F. Meijers, S. Mersi, E. Meschi, F. Moortgat, S. Morovic, M. Mulders, M.V. Nemallapudi, H. Neugebauer, S. Orfanelli⁴¹, L. Orsini, L. Pape, E. Perez, A. Petrilli, G. Petrucciani, A. Pfeiffer, D. Piparo, A. Racz, G. Rolandi⁴², M. Rovere, M. Ruan, H. Sakulin, C. Schäfer, C. Schwick, A. Sharma, P. Silva, M. Simon, P. Sphicas⁴³, D. Spiga, J. Steggemann, B. Stieger, M. Stoye, Y. Takahashi, D. Treille, A. Triossi, A. Tsiros, G.I. Veres²⁰, N. Wardle, H.K. Wöhri, A. Zagozdinska⁴⁴, W.D. Zeuner

CERN, European Organization for Nuclear Research, Geneva, Switzerland

W. Bertl, K. Deiters, W. Erdmann, R. Horisberger, Q. Ingram, H.C. Kaestli, D. Kotlinski, U. Langenegger, D. Renker, T. Rohe

Paul Scherrer Institut, Villigen, Switzerland

F. Bachmair, L. Bäni, L. Bianchini, M.A. Buchmann, B. Casal, G. Dissertori, M. Dittmar, M. Donegà, M. Dünser, P. Eller, C. Grab, C. Heidegger, D. Hits, J. Hoss, G. Kasieczka, W. Lustermann, B. Mangano, A.C. Marini, M. Marionneau, P. Martinez Ruiz del Arbol, M. Masciovecchio, D. Meister, P. Musella,

F. Nessi-Tedaldi, F. Pandolfi, J. Pata, F. Pauss, L. Perrozzi, M. Peruzzi, M. Quittnat, M. Rossini, A. Starodumov⁴⁵, M. Takahashi, V.R. Tavolaro, K. Theofilatos, R. Wallny

Institute for Particle Physics, ETH Zurich, Zurich, Switzerland

T.K. Aarrestad, C. Amsler⁴⁶, L. Caminada, M.F. Canelli, V. Chiochia, A. De Cosa, C. Galloni, A. Hinzmann, T. Hreus, B. Kilminster, C. Lange, J. Ngadiuba, D. Pinna, P. Robmann, F.J. Ronga, D. Salerno, Y. Yang

Universität Zürich, Zurich, Switzerland

M. Cardaci, K.H. Chen, T.H. Doan, C. Ferro, Sh. Jain, R. Khurana, M. Konyushikhin, C.M. Kuo, W. Lin, Y.J. Lu, R. Volpe, S.S. Yu

National Central University, Chung-Li, Taiwan

R. Bartek, P. Chang, Y.H. Chang, Y.W. Chang, Y. Chao, K.F. Chen, P.H. Chen, C. Dietz, F. Fiori, U. Grundler, W.-S. Hou, Y. Hsiung, Y.F. Liu, R.-S. Lu, M. Miñano Moya, E. Petrakou, J.F. Tsai, Y.M. Tzeng

National Taiwan University (NTU), Taipei, Taiwan

B. Asavapibhop, K. Kovitanggoon, G. Singh, N. Srimanobhas, N. Suwonjandee

Chulalongkorn University, Faculty of Science, Department of Physics, Bangkok, Thailand

A. Adiguzel, M.N. Bakirci⁴⁷, C. Dozen, I. Dumanoglu, E. Eskut, S. Girgis, G. Gokbulut, Y. Guler, E. Gurpinar, I. Hos, E.E. Kangal⁴⁸, G. Onengut⁴⁹, K. Ozdemir⁵⁰, A. Polatoz, D. Sunar Cerci⁵¹, M. Vergili, C. Zorbilmez

Cukurova University, Adana, Turkey

I.V. Akin, B. Bilin, S. Bilmis, B. Isildak⁵², G. Karapinar⁵³, U.E. Surat, M. Yalvac, M. Zeyrek

Middle East Technical University, Physics Department, Ankara, Turkey

E.A. Albayrak⁵⁴, E. Gülmez, M. Kaya⁵⁵, O. Kaya⁵⁶, T. Yetkin⁵⁷

Bogazici University, Istanbul, Turkey

K. Cankocak, S. Sen⁵⁸, F.I. Vardarli

Istanbul Technical University, Istanbul, Turkey

B. Grynyov

Institute for Scintillation Materials of National Academy of Science of Ukraine, Kharkov, Ukraine

L. Levchuk, P. Sorokin

National Scientific Center, Kharkov Institute of Physics and Technology, Kharkov, Ukraine

R. Aggleton, F. Ball, L. Beck, J.J. Brooke, E. Clement, D. Cussans, H. Flacher, J. Goldstein, M. Grimes, G.P. Heath, H.F. Heath, J. Jacob, L. Kreczko, C. Lucas, Z. Meng, D.M. Newbold⁵⁹, S. Paramesvaran, A. Poll, T. Sakuma, S. Seif El Nasr-storey, S. Senkin, D. Smith, V.J. Smith

University of Bristol, Bristol, United Kingdom

K.W. Bell, A. Belyaev⁶⁰, C. Brew, R.M. Brown, D.J.A. Cockerill, J.A. Coughlan, K. Harder, S. Harper, E. Olaiya, D. Petyt, C.H. Shepherd-Themistocleous, A. Thea, L. Thomas, I.R. Tomalin, T. Williams, W.J. Womersley, S.D. Worm

Rutherford Appleton Laboratory, Didcot, United Kingdom

M. Baber, R. Bainbridge, O. Buchmuller, A. Bundock, D. Burton, S. Casasso, M. Citron, D. Colling, L. Corpe, N. Cripps, P. Dauncey, G. Davies, A. De Wit, M. Della Negra, P. Dunne, A. Elwood, W. Ferguson, J. Fulcher, D. Futyan, G. Hall, G. Iles, G. Karapostoli, M. Kenzie, R. Lane, R. Lucas⁵⁹, L. Lyons, A.-M. Magnan,

S. Malik, J. Nash, A. Nikitenko⁴⁵, J. Pela, M. Pesaresi, K. Petridis, D.M. Raymond, A. Richards, A. Rose, C. Seez, A. Tapper, K. Uchida, M. Vazquez Acosta⁶¹, T. Virdee, S.C. Zenz

Imperial College, London, United Kingdom

J.E. Cole, P.R. Hobson, A. Khan, P. Kyberd, D. Leggat, D. Leslie, I.D. Reid, P. Symonds, L. Teodorescu, M. Turner

Brunel University, Uxbridge, United Kingdom

A. Borzou, K. Call, J. Dittmann, K. Hatakeyama, A. Kasmi, H. Liu, N. Pastika

Baylor University, Waco, USA

O. Charaf, S.I. Cooper, C. Henderson, P. Rumerio

The University of Alabama, Tuscaloosa, USA

A. Avetisyan, T. Bose, C. Fantasia, D. Gastler, P. Lawson, D. Rankin, C. Richardson, J. Rohlf, J. St. John, L. Sulak, D. Zou

Boston University, Boston, USA

J. Alimena, E. Berry, S. Bhattacharya, D. Cutts, N. Dhingra, A. Ferapontov, A. Garabedian, U. Heintz, E. Laird, G. Landsberg, Z. Mao, M. Narain, S. Sagir, T. Sinthuprasith

Brown University, Providence, USA

R. Breedon, G. Breto, M. Calderon De La Barca Sanchez, S. Chauhan, M. Chertok, J. Conway, R. Conway, P.T. Cox, R. Erbacher, M. Gardner, W. Ko, R. Lander, M. Mulhearn, D. Pellett, J. Pilot, F. Ricci-Tam, S. Shalhout, J. Smith, M. Squires, D. Stolp, M. Tripathi, S. Wilbur, R. Yohay

University of California, Davis, Davis, USA

R. Cousins, P. Everaerts, C. Farrell, J. Hauser, M. Ignatenko, D. Saltzberg, E. Takasugi, V. Valuev, M. Weber

University of California, Los Angeles, USA

K. Burt, R. Clare, J. Ellison, J.W. Gary, G. Hanson, J. Heilman, M. Ivova Paneva, P. Jandir, E. Kennedy, F. Lacroix, O.R. Long, A. Luthra, M. Malberti, M. Olmedo Negrete, A. Shrinivas, H. Wei, S. Wimpenny

University of California, Riverside, Riverside, USA

J.G. Branson, G.B. Cerati, S. Cittolin, R.T. D'Agnolo, A. Holzner, R. Kelley, D. Klein, J. Letts, I. Macneill, D. Olivito, S. Padhi, M. Pieri, M. Sani, V. Sharma, S. Simon, M. Tadel, A. Vartak, S. Wasserbaech⁶², C. Welke, F. Würthwein, A. Yagil, G. Zevi Della Porta

University of California, San Diego, La Jolla, USA

D. Barge, J. Bradmiller-Feld, C. Campagnari, A. Dishaw, V. Dutta, K. Flowers, M. Franco Sevilla, P. Geffert, C. George, F. Golf, L. Gouskos, J. Gran, J. Incandela, C. Justus, N. Mccoll, S.D. Mullin, J. Richman, D. Stuart, I. Suarez, W. To, C. West, J. Yoo

University of California, Santa Barbara, Santa Barbara, USA

D. Anderson, A. Apresyan, A. Bornheim, J. Bunn, Y. Chen, J. Duarte, A. Mott, H.B. Newman, C. Pena, M. Pierini, M. Spiropulu, J.R. Vlimant, S. Xie, R.Y. Zhu

California Institute of Technology, Pasadena, USA

V. Azzolini, A. Calamba, B. Carlson, T. Ferguson, Y. Iiyama, M. Paulini, J. Russ, M. Sun, H. Vogel, I. Vorobiev

Carnegie Mellon University, Pittsburgh, USA

J.P. Cumalat, W.T. Ford, A. Gaz, F. Jensen, A. Johnson, M. Krohn, T. Mulholland, U. Nauenberg, J.G. Smith, K. Stenson, S.R. Wagner

University of Colorado Boulder, Boulder, USA

J. Alexander, A. Chatterjee, J. Chaves, J. Chu, S. Dittmer, N. Eggert, N. Mirman, G. Nicolas Kaufman, J.R. Patterson, A. Rinkevicius, A. Ryd, L. Skinnari, L. Soffi, W. Sun, S.M. Tan, W.D. Teo, J. Thom, J. Thompson, J. Tucker, Y. Weng, P. Wittich

Cornell University, Ithaca, USA

S. Abdullin, M. Albrow, J. Anderson, G. Apollinari, L.A.T. Bauerdick, A. Beretvas, J. Berryhill, P.C. Bhat, G. Bolla, K. Burkett, J.N. Butler, H.W.K. Cheung, F. Chlebana, S. Cihangir, V.D. Elvira, I. Fisk, J. Freeman, E. Gottschalk, L. Gray, D. Green, S. Grünendahl, O. Gutsche, J. Hanlon, D. Hare, R.M. Harris, J. Hirschauer, B. Hooberman, Z. Hu, S. Jindariani, M. Johnson, U. Joshi, A.W. Jung, B. Klima, B. Kreis, S. Kwan[†], S. Lammel, J. Linacre, D. Lincoln, R. Lipton, T. Liu, R. Lopes De Sá, J. Lykken, K. Maeshima, J.M. Marraffino, V.I. Martinez Outschoorn, S. Maruyama, D. Mason, P. McBride, P. Merkel, K. Mishra, S. Mrenna, S. Nahn, C. Newman-Holmes, V. O'Dell, K. Pedro, O. Prokofyev, G. Rakness, E. Sexton-Kennedy, A. Soha, W.J. Spalding, L. Spiegel, L. Taylor, S. Tkaczyk, N.V. Tran, L. Uplegger, E.W. Vaandering, C. Vernieri, M. Verzocchi, R. Vidal, H.A. Weber, A. Whitbeck, F. Yang, H. Yin

Fermi National Accelerator Laboratory, Batavia, USA

D. Acosta, P. Avery, P. Bortignon, D. Bourilkov, A. Carnes, M. Carver, D. Curry, S. Das, G.P. Di Giovanni, R.D. Field, M. Fisher, I.K. Furic, J. Hugon, J. Konigsberg, A. Korytov, J.F. Low, P. Ma, K. Matchev, H. Mei, P. Milenovic⁶³, G. Mitselmakher, L. Muniz, D. Rank, R. Rossin, L. Shchutska, M. Snowball, D. Sperka, J. Wang, S. Wang, J. Yelton

University of Florida, Gainesville, USA

S. Hewamanage, S. Linn, P. Markowitz, G. Martinez, J.L. Rodriguez

Florida International University, Miami, USA

A. Ackert, J.R. Adams, T. Adams, A. Askew, J. Bochenek, B. Diamond, J. Haas, S. Hagopian, V. Hagopian, K.F. Johnson, A. Khatiwada, H. Prosper, V. Veeraraghavan, M. Weinberg

Florida State University, Tallahassee, USA

M.M. Baarmand, V. Bhopatkar, M. Hohlmann, H. Kalakhety, D. Mareskas-palcek, T. Roy, F. Yumiceva

Florida Institute of Technology, Melbourne, USA

M.R. Adams, L. Apanasevich, D. Berry, R.R. Betts, I. Bucinskaite, R. Cavanaugh, O. Evdokimov, L. Gauthier, C.E. Gerber, D.J. Hofman, P. Kurt, C. O'Brien, I.D. Sandoval Gonzalez, C. Silkworth, P. Turner, N. Varelas, Z. Wu, M. Zakaria

University of Illinois at Chicago (UIC), Chicago, USA

B. Bilki⁶⁴, W. Clarida, K. Dilsiz, S. Durgut, R.P. Gandrajula, M. Haytmyradov, V. Khristenko, J.-P. Merlo, H. Mermerkaya⁶⁵, A. Mestvirishvili, A. Moeller, J. Nachtman, H. Ogul, Y. Onel, F. Ozok⁵⁴, A. Penzo, C. Snyder, P. Tan, E. Tiras, J. Wetzel, K. Yi

The University of Iowa, Iowa City, USA

I. Anderson, B.A. Barnett, B. Blumenfeld, D. Fehling, L. Feng, A.V. Gritsan, P. Maksimovic, C. Martin, M. Osherson, M. Swartz, M. Xiao, Y. Xin, C. You

Johns Hopkins University, Baltimore, USA

P. Baringer, A. Bean, G. Benelli, C. Bruner, J. Gray, R.P. Kenny III, D. Majumder, M. Malek, M. Murray, D. Noonan, S. Sanders, R. Stringer, Q. Wang, J.S. Wood

The University of Kansas, Lawrence, USA

I. Chakaberia, A. Ivanov, K. Kaadze, S. Khalil, M. Makouski, Y. Maravin, A. Mohammadi, L.K. Saini, N. Skhirtladze, I. Svintradze, S. Toda

Kansas State University, Manhattan, USA

D. Lange, F. Rebassoo, D. Wright

Lawrence Livermore National Laboratory, Livermore, USA

C. Anelli, A. Baden, O. Baron, A. Belloni, B. Calvert, S.C. Eno, C. Ferraioli, J.A. Gomez, N.J. Hadley, S. Jabeen, R.G. Kellogg, T. Kolberg, J. Kunkle, Y. Lu, A.C. Mignerey, Y.H. Shin, A. Skuja, M.B. Tonjes, S.C. Tonwar

University of Maryland, College Park, USA

A. Apyan, R. Barbieri, A. Baty, K. Bierwagen, S. Brandt, W. Busza, I.A. Cali, Z. Demiragli, L. Di Matteo, G. Gomez Ceballos, M. Goncharov, D. Gulhan, G.M. Innocenti, M. Klute, D. Kovalskyi, Y.S. Lai, Y.-J. Lee, A. Levin, P.D. Luckey, C. McGinn, C. Mironov, X. Niu, C. Paus, D. Ralph, C. Roland, G. Roland, J. Salfeld-Nebgen, G.S.F. Stephans, K. Sumorok, M. Varma, D. Velicanu, J. Veverka, J. Wang, T.W. Wang, B. Wyslouch, M. Yang, V. Zhukova

Massachusetts Institute of Technology, Cambridge, USA

B. Dahmes, A. Finkel, A. Gude, P. Hansen, S. Kalafut, S.C. Kao, K. Klapoetke, Y. Kubota, Z. Lesko, J. Mans, S. Nourbakhsh, N. Ruckstuhl, R. Rusack, N. Tambe, J. Turkewitz

University of Minnesota, Minneapolis, USA

J.G. Acosta, S. Oliveros

University of Mississippi, Oxford, USA

E. Avdeeva, K. Bloom, S. Bose, D.R. Claes, A. Dominguez, C. Fangmeier, R. Gonzalez Suarez, R. Kamalieddin, J. Keller, D. Knowlton, I. Kravchenko, J. Lazo-Flores, F. Meier, J. Monroy, F. Ratnikov, J.E. Siado, G.R. Snow

University of Nebraska—Lincoln, Lincoln, USA

M. Alyari, J. Dolen, J. George, A. Godshalk, I. Iashvili, J. Kaisen, A. Kharchilava, A. Kumar, S. Rappoccio

State University of New York at Buffalo, Buffalo, USA

G. Alverson, E. Barberis, D. Baumgartel, M. Chasco, A. Hortiangtham, A. Massironi, D.M. Morse, D. Nash, T. Orimoto, R. Teixeira De Lima, D. Trocino, R.-J. Wang, D. Wood, J. Zhang

Northeastern University, Boston, USA

K.A. Hahn, A. Kubik, N. Mucia, N. Odell, B. Pollack, A. Pozdnyakov, M. Schmitt, S. Stoynev, K. Sung, M. Trovato, M. Velasco, S. Won

Northwestern University, Evanston, USA

A. Brinkerhoff, N. Dev, M. Hildreth, C. Jessop, D.J. Karmgard, N. Kellams, K. Lannon, S. Lynch, N. Marinelli, F. Meng, C. Mueller, Y. Musienko³⁵, T. Pearson, M. Planer, A. Reinsvold, R. Ruchti, G. Smith, S. Taroni, N. Valls, M. Wayne, M. Wolf, A. Woodard

University of Notre Dame, Notre Dame, USA

L. Antonelli, J. Brinson, B. Bylsma, L.S. Durkin, S. Flowers, A. Hart, C. Hill, R. Hughes, K. Kotov, T.Y. Ling, B. Liu, W. Luo, D. Puigh, M. Rodenburg, B.L. Winer, H.W. Wulsin

The Ohio State University, Columbus, USA

O. Driga, P. Elmer, J. Hardenbrook, P. Hebda, S.A. Koay, P. Lujan, D. Marlow, T. Medvedeva, M. Mooney, J. Olsen, C. Palmer, P. Piroué, X. Quan, H. Saka, D. Stickland, C. Tully, J.S. Werner, A. Zuranski

Princeton University, Princeton, USA

V.E. Barnes, D. Benedetti, D. Bortoletto, L. Gutay, M.K. Jha, M. Jones, K. Jung, M. Kress, D.H. Miller, N. Neumeister, F. Primavera, B.C. Radburn-Smith, X. Shi, I. Shipsey, D. Silvers, J. Sun, A. Svyatkovskiy, F. Wang, W. Xie, L. Xu, J. Zablocki

Purdue University, West Lafayette, USA

N. Parashar, J. Stupak

Purdue University Calumet, Hammond, USA

A. Adair, B. Akgun, Z. Chen, K.M. Ecklund, F.J.M. Geurts, M. Guilbaud, W. Li, B. Michlin, M. Northup, B.P. Padley, R. Redjimi, J. Roberts, J. Rorie, Z. Tu, J. Zabel

Rice University, Houston, USA

B. Betchart, A. Bodek, P. de Barbaro, R. Demina, Y. Eshaq, T. Ferbel, M. Galanti, A. Garcia-Bellido, P. Goldenzweig, J. Han, A. Harel, O. Hindrichs, A. Khukhunaishvili, G. Petrillo, M. Verzetti

University of Rochester, Rochester, USA

L. Demortier

The Rockefeller University, New York, USA

S. Arora, A. Barker, J.P. Chou, C. Contreras-Campana, E. Contreras-Campana, D. Duggan, D. Ferencek, Y. Gershtein, R. Gray, E. Halkiadakis, D. Hidas, E. Hughes, S. Kaplan, R. Kunnawalkam Elayavalli, A. Lath, K. Nash, S. Panwalkar, M. Park, S. Salur, S. Schnetzer, D. Sheffield, S. Somalwar, R. Stone, S. Thomas, P. Thomassen, M. Walker

Rutgers, The State University of New Jersey, Piscataway, USA

M. Foerster, G. Riley, K. Rose, S. Spanier, A. York

University of Tennessee, Knoxville, USA

O. Bouhali⁶⁶, A. Castaneda Hernandez, M. Dalchenko, M. De Mattia, A. Delgado, S. Dildick, R. Eusebi, W. Flanagan, J. Gilmore, T. Kamon⁶⁷, V. Krutelyov, R. Montalvo, R. Mueller, I. Osipenkov, Y. Pakhotin, R. Patel, A. Perloff, J. Roe, A. Rose, A. Safonov, A. Tatarinov, K.A. Ulmer²

Texas A&M University, College Station, USA

N. Akchurin, C. Cowden, J. Damgov, C. Dragoiu, P.R. Duderov, J. Faulkner, S. Kunori, K. Lamichhane, S.W. Lee, T. Libeiro, S. Undleeb, I. Volobouev

Texas Tech University, Lubbock, USA

E. Appelt, A.G. Delannoy, S. Greene, A. Gurrola, R. Janjam, W. Johns, C. Maguire, Y. Mao, A. Melo, P. Sheldon, B. Snook, S. Tuo, J. Velkovska, Q. Xu

Vanderbilt University, Nashville, USA

M.W. Arenton, S. Boutle, B. Cox, B. Francis, J. Goodell, R. Hirosky, A. Ledovskoy, H. Li, C. Lin, C. Neu, E. Wolfe, J. Wood, F. Xia

University of Virginia, Charlottesville, USA

C. Clarke, R. Harr, P.E. Karchin, C. Kottachchi Kankanamge Don, P. Lamichhane, J. Sturdy

Wayne State University, Detroit, USA

D.A. Belknap, D. Carlsmith, M. Cepeda, A. Christian, S. Dasu, L. Dodd, S. Duric, E. Friis, B. Gomber, R. Hall-Wilton, M. Herndon, A. Hervé, P. Klabbbers, A. Lanaro, A. Levine, K. Long, R. Loveless, A. Mohapatra, I. Ojalvo, T. Perry, G.A. Pierro, G. Polese, I. Ross, T. Ruggles, T. Sarangi, A. Savin, A. Sharma, N. Smith, W.H. Smith, D. Taylor, N. Woods

University of Wisconsin, Madison, USA

[†] Deceased.

- ¹ Also at Vienna University of Technology, Vienna, Austria.
- ² Also at CERN, European Organization for Nuclear Research, Geneva, Switzerland.
- ³ Also at State Key Laboratory of Nuclear Physics and Technology, Peking University, Beijing, China.
- ⁴ Also at Institut Pluridisciplinaire Hubert Curien, Université de Strasbourg, Université de Haute Alsace Mulhouse, CNRS/IN2P3, Strasbourg, France.
- ⁵ Also at National Institute of Chemical Physics and Biophysics, Tallinn, Estonia.
- ⁶ Also at Skobel'syn Institute of Nuclear Physics, Lomonosov Moscow State University, Moscow, Russia.
- ⁷ Also at Universidade Estadual de Campinas, Campinas, Brazil.
- ⁸ Also at Centre National de la Recherche Scientifique (CNRS) – IN2P3, Paris, France.
- ⁹ Also at Laboratoire Leprince-Ringuet, Ecole Polytechnique, IN2P3–CNRS, Palaiseau, France.
- ¹⁰ Also at Joint Institute for Nuclear Research, Dubna, Russia.
- ¹¹ Also at Zewail City of Science and Technology, Zewail, Egypt.
- ¹² Also at Ain Shams University, Cairo, Egypt.
- ¹³ Now at British University in Egypt, Cairo, Egypt.
- ¹⁴ Also at Helwan University, Cairo, Egypt.
- ¹⁵ Also at Université de Haute Alsace, Mulhouse, France.
- ¹⁶ Also at Tbilisi State University, Tbilisi, Georgia.
- ¹⁷ Also at Ilia State University, Tbilisi, Georgia.
- ¹⁸ Also at Brandenburg University of Technology, Cottbus, Germany.
- ¹⁹ Also at Institute of Nuclear Research ATOMKI, Debrecen, Hungary.
- ²⁰ Also at Eötvös Loránd University, Budapest, Hungary.
- ²¹ Also at University of Debrecen, Debrecen, Hungary.
- ²² Also at Wigner Research Centre for Physics, Budapest, Hungary.
- ²³ Also at University of Visva-Bharati, Santiniketan, India.
- ²⁴ Now at King Abdulaziz University, Jeddah, Saudi Arabia.
- ²⁵ Also at University of Ruhuna, Matara, Sri Lanka.
- ²⁶ Also at Isfahan University of Technology, Isfahan, Iran.
- ²⁷ Also at University of Tehran, Department of Engineering Science, Tehran, Iran.
- ²⁸ Also at Plasma Physics Research Center, Science and Research Branch, Islamic Azad University, Tehran, Iran.
- ²⁹ Also at Laboratori Nazionali di Legnaro dell'INFN, Legnaro, Italy.
- ³⁰ Also at Università degli Studi di Siena, Siena, Italy.
- ³¹ Also at Purdue University, West Lafayette, USA.
- ³² Also at International Islamic University of Malaysia, Kuala Lumpur, Malaysia.
- ³³ Also at Malaysian Nuclear Agency, Mosti, Kajang, Malaysia.
- ³⁴ Also at Consejo Nacional de Ciencia y Tecnología, Mexico, Mexico.
- ³⁵ Also at Institute for Nuclear Research, Moscow, Russia.
- ³⁶ Also at St. Petersburg State Polytechnical University, St. Petersburg, Russia.
- ³⁷ Also at National Research Nuclear University 'Moscow Engineering Physics Institute' (MEPhI), Moscow, Russia.
- ³⁸ Also at California Institute of Technology, Pasadena, USA.
- ³⁹ Also at Faculty of Physics, University of Belgrade, Belgrade, Serbia.
- ⁴⁰ Also at Facoltà Ingegneria, Università di Roma, Roma, Italy.
- ⁴¹ Also at National Technical University of Athens, Athens, Greece.
- ⁴² Also at Scuola Normale e Sezione dell'INFN, Pisa, Italy.
- ⁴³ Also at University of Athens, Athens, Greece.
- ⁴⁴ Also at Warsaw University of Technology, Institute of Electronic Systems, Warsaw, Poland.
- ⁴⁵ Also at Institute for Theoretical and Experimental Physics, Moscow, Russia.
- ⁴⁶ Also at Albert Einstein Center for Fundamental Physics, Bern, Switzerland.
- ⁴⁷ Also at Gaziosmanpasa University, Tokat, Turkey.
- ⁴⁸ Also at Mersin University, Mersin, Turkey.
- ⁴⁹ Also at Cag University, Mersin, Turkey.
- ⁵⁰ Also at Piri Reis University, Istanbul, Turkey.
- ⁵¹ Also at Adiyaman University, Adiyaman, Turkey.
- ⁵² Also at Ozyegin University, Istanbul, Turkey.
- ⁵³ Also at Izmir Institute of Technology, Izmir, Turkey.
- ⁵⁴ Also at Mimar Sinan University, Istanbul, Istanbul, Turkey.
- ⁵⁵ Also at Marmara University, Istanbul, Turkey.
- ⁵⁶ Also at Kafkas University, Kars, Turkey.
- ⁵⁷ Also at Yildiz Technical University, Istanbul, Turkey.
- ⁵⁸ Also at Hacettepe University, Ankara, Turkey.
- ⁵⁹ Also at Rutherford Appleton Laboratory, Didcot, United Kingdom.
- ⁶⁰ Also at School of Physics and Astronomy, University of Southampton, Southampton, United Kingdom.

⁶¹ Also at Instituto de Astrofísica de Canarias, La Laguna, Spain.

⁶² Also at Utah Valley University, Orem, USA.

⁶³ Also at University of Belgrade, Faculty of Physics and Vinca Institute of Nuclear Sciences, Belgrade, Serbia.

⁶⁴ Also at Argonne National Laboratory, Argonne, USA.

⁶⁵ Also at Erzincan University, Erzincan, Turkey.

⁶⁶ Also at Texas A&M University at Qatar, Doha, Qatar.

⁶⁷ Also at Kyungpook National University, Daegu, Republic of Korea.